E-ISSN: 3108-4672

INHERITED METABOLIC DISORDERS AND NUTRITION

Volume: 2 | 2026



https://imdnjournal.com/

galenos yayinevi

INHERITED METABOLIC DISORDERS AND NUTRITION

Editorial Board

Editor in Chief

PhD, M.D., Prof. Nur Arslan

Dokuz Eylül University Faculty of Medicine, Department of Pediatrics, Division of Pediatric Metabolism, İzmir, Türkiye

E-mail: nur.arslan@deu.edu.tr

ORCID-ID: 0000-0003-3151-3741

Editors

PhD, M.D., Prof. Saadet Andrews

University of Alberta, Faculty of Medicine and Dentistry, College of Health Sciences, Department of Medical Genetics, Edmonton, Canada

E-mail: saadet@ualberta.ca

ORCID-ID: 0000-0001-8396-6764

M.D., Assoc. Prof. Mehmet Gündüz

Health Sciences University Türkiye, Ankara Bilkent City Hospital, Clinic of Pediatrics, Division of Metabolism and Nutrition, Ankara, Türkiye

E-mail: mehmetgunduz52@yahoo.com

ORCID-ID: 0000-0002-6005-5623

PhD, M.D., Prof. Johannes Häberle

Kinderspital Zurich, University Children's Hospital, Clinic of Metabolism, Zurich, Switzerland

E-mail: Johannes.haeberle@kispi.uzh.ch

ORCID-ID: 0000-0003-0635-091X

M.D., Assoc. Prof. Burcu Öztürk Hişmi

Marmara University Faculty of Medicine, Department of Pediatrics, Division of Pediatric Metabolic Disorders, İstanbul, Türkiye

E-mail: 0000-0001-7146-0248

M.D., Prof. Fatih Kardaş

Erciyes University Faculty of Medicine, Department of Pediatrics, Division of Pediatric Nutrition and Metabolism, Kayseri, Türkiye

E-mail: fkardas@erciyes.edu.tr

ORCID-ID: 0000-0002-2276-7611

M.D., Prof. Ertuğrul Kıykım

İstanbul University-Cerrahpaşa, Cerrahpaşa Faculty of Medicine, Department of Pediatrics, Division of Nutrition and Metabolism, İstanbul, Türkiye

E-mail: ertugrul.kiykim@iuc.edu.tr

ORCID-ID: 0000-0001-5170-5594

M.D., Prof. Sema Kalkan Uçar

Ege University Faculty of Medicine, Department of Pediatrics, Division of Metabolism and Nutrition, İzmir, Türkiye

E-mail: sema.kalkan.ucar@ege.edu.tr

ORCID-ID: 0000-0001-9574-7841

M.D., Prof. Özlem Ünal Uzun

Kocaeli University Faculty of Medicine, Department of Pediatrics, Division of Pediatric Metabolism, Kocaeli, Türkiye

E-mail: unalozlem@gmail.com

ORCID-ID: 0000-0001-7937-7721

PhD, M.D., Prof. Saskia B. Wortmann

Salzburger Landeskliniken and Paracelsus Medical University, Department of Pediatrics, Salzburg, Austria Amalia Children's Hospital, Radboud University Medical Center for Mitochondrial and Metabolic Medicine, Department of Pediatrics, Nijmegen, Netherlands

E-mail: s.wortmann@salk.at

ORCID-ID: 0000-0002-1968-8103

Please refer to the journal's webpage (https://imdnjournal.com/) for "Journal Policy", and "Instructions to Authors".

Inherited Metabolic Disorders and Nutrition and its editors follow the recommendations of "International Committee of Medical Journal Editors (ICMJE)", "World Association of Medical Editors (WAME)", "Council of Science Editors (CSE)", "Committee on Publication Ethics (COPE)", "European Association of Science Editors (EASE)", and "National Information Standards Organization (NISO)."

The journal is published online.

Owner: Child Nutrition and Metabolism Association

Responsible Manager: Nur Arslan

Publisher Contact
Address: Molla Gürani Mah. Kaçamak Sk. No: 21/1 34093 İstanbul, Türkiye
Phone: +90 (530) 177 30 97 / +90 (539) 307 32 03
E-mail: info@galenos.com.tr • yayin@galenos.com.tr
Web: www.galenos.com.tr

Publisher Certificate Number: 14521
E-ISSN: 3108-4672

INHERITED METABOLIC DISORDERS AND NUTRITION

Editorial

Dear Colleagues,

We are delighted to announce the launch of the inaugural issue of Inherited Metabolic Disorders and Nutrition (IMDN), the official journal of the Child Nutrition and Metabolism Association. The journal provides a platform for academics to advance scientific research, report rare case studies, and share innovative ideas - all contributing to the growing body of knowledge in our field.

Inherited metabolic disorders represent a critical area of research, with an increasing number of researchers and publications dedicated to this field worldwide. IMDN was established in response to the ongoing need for additional avenues to publish high-quality research in this area. The journal aspires to make a lasting contribution to the fields of paediatric nutrition and inherited metabolic disorders. With the release of the first issue, a strong commitment is renewed to position IMDN as a leading resource within the international scientific community. Over time, we hope that IMDN will become an essential tool for sharing information and experiences related to metabolic disorders and nutrition.

IMDN will be published quarterly and will feature peer-reviewed research articles, case reports, reviews, original studies, and other relevant content. Our editorial board comprises experts from around the globe, and we welcome contributions from our international colleagues.

For more information about IMDN, please visit our website at www.imdn.org. I encourage you to read the first issue with great interest, and I extend my sincere thanks to the authors whose work is featured in it. As a newly established journal, IMDN will undoubtedly thrive with your continued support and contributions.

We look forward to receiving your submissions for future issues.

Best regards,

Nur Arslan
Editor-in-Chief

ORIGINAL ARTICLE

DOI: 10.4274/imdn.galenos.2025.2025-4

Inherit Metab Disord Nutr 2026;2:1–6

Development and Validation of a Multiplex LC-MS/MS Assay for Lysosphingolipid Quantification in the Diagnosis of Gaucher and Fabry Diseases

Halide Akbaş[1], Ayşe Ergül Bozacı[2] , Bilge Karatoy Erdem[1], Nurullah Özsarı[3], Erdoğan Soyuçen[2]

[1]Akdeniz University Faculty of Medicine, Department of Biochemistry, Antalya, Türkiye

[2]Akdeniz University Faculty of Medicine, Department of Pediatric Metabolism, Antalya, Türkiye

[3]Bilecik Research and Training Hospital, Clinic of Biochemistry, Bilecik, Türkiye

Abstract

Objectives: Lysosphingolipids (LysoSLs), the N-deacylated forms of sphingolipids, are increasingly recognized as toxic metabolites that accumulate in various lysosomal storage disorders (LSDs), collectively known as sphingolipidoses. These compounds, due to their amphiphilic nature and bioactive properties, can contribute to cellular dysfunction and disease pathogenesis. Recent studies have demonstrated that specific LysoSLs, such as hexosylsphingosine (HexSph), globotriaosylsphingosine (LysoGb3), and lysosphingomyelin (LysoSM), are elevated in plasma, serum, or dried blood spots from patients with Gaucher, Fabry, Krabbe, or Niemann-Pick diseases. These findings have paved the way for the use of LysoSLs as sensitive and specific biomarkers in the diagnosis, prognosis, and therapeutic monitoring of sphingolipidoses. This study aimed to develop and validate a method for the simultaneous quantification of three LysoSLs—HexSph, LysoGb3, and LysoSM—using liquid chromatography–tandem mass spectrometry (LC-MS/MS), for use in the diagnosis and follow-up of sphingolipidoses.

Materials and Methods: A multiplex analytical method was optimized for quantifying HexSph, LysoGb3, and LysoSM by ultra-fast LC coupled to tandem MS (UFLC-MS/MS) in positive-ion mode with electrospray ionization (LC-20 AD UFLC XR; Shimadzu 8040, Japan), employing multiple reaction monitoring. The method was validated for linearity, accuracy, precision, limit of detection, limit of quantification, and recovery rates. Following method validation, plasma samples were collected from 14 patients diagnosed with Gaucher disease or Fabry disease at Akdeniz University Hospital and from 20 healthy adult volunteers. Sample preparation involved methanol/acetone/water extraction prior to analysis of LysoSL concentrations.

Results: The total analysis time for all three analytes was determined to be 10 minutes. Calibration curves demonstrated strong linearity, with coefficients of determination (r^2) of 0.995 for LysoSM, 0.982 for HexSph, and 0.961 for LysoGb3. Plasma concentrations of LysoSLs were measured in both the patient and control groups. Significantly elevated levels of LysoSM and HexSph were observed in Gaucher patients compared to healthy controls. While LysoGb3 levels were higher in Fabry patients than in controls, the difference did not reach statistical significance.

Conclusion: This validated multiplex LC-MS/MS assay enables rapid and reliable simultaneous quantification of key LysoSLs in plasma. The assay holds promise as a diagnostic and monitoring tool for sphingolipidoses and may be further expanded to include additional biomarkers relevant to other LSDs. Quantification of LysoSLs can support clinical decision-making, including therapeutic selection and monitoring of patients undergoing enzyme replacement therapy.

Keywords: Lysosphingolipid, Hexosylsphingosine, Globotriaosylsphingosine, Lysosphingomyelin, LC-MS/MS

Address for Correspondence: Ayşe Ergül Bozacı, Akdeniz University Faculty of Medicine, Department of Pediatric Metabolism, Antalya, Türkiye

E-mail: ergul.acar@yahoo.com.tr **ORCID ID:** orcid.org/0000-0002-9783-1016

Received: 12.09.2025 **Accepted:** 22.12.2025 **Epub:** 26.12.2025 **Publication Date:** 12.01.2026

Cite this article as: Akbaş H, Ergül Bozacı A , Karatoy Erdem B, Özsarı N, Soyuçen E. Development and validation of a multiplex LC–MS/MS assay for lysosphingolipid quantification in the diagnosis of Gaucher and Fabry diseases. Inherit Metab Disord Nutr. 2026;2:1–6

Copyright© 2026 The Author(s). Published by Galenos Publishing House on behalf of Child Nutrition Metabolism Association.
This is an open access article under the Creative Commons AttributionNonCommercial 4.0 International (CC BY-NC 4.0) License.

INTRODUCTION

Sphingolipidoses are a subgroup of lysosomal storage disorders (LSDs) caused by inherited defects in lysosomal degradation pathways of sphingolipids.[1,2] This group of inborn metabolic diseases includes primary sphingolipidoses, such as Niemann-Pick types A, B, and A/B (NPA/B), Fabry disease (FD), Krabbe disease (KD), Gaucher disease (GD), and Tay-Sachs disease, all of which are caused by mutations in genes encoding specific lysosomal enzymes. Secondary sphingolipidoses, such as NPC, as well as disorders related to saposin deficiencies, are included.

Due to overlapping clinical manifestations among various sphingolipidoses, accurate clinical diagnosis is often challenging. Therefore, identification and analysis of molecular biomarkers that can facilitate differential diagnoses have become increasingly important. Liquid chromatography–tandem mass spectrometry (LC-MS/MS) is a widely used, highly sensitive, and highly specific analytical technique for biomarker quantification. One of its key advantages is the ability to simultaneously measure multiple analytes within a single run.

In recent years, the metabolism and biological functions of sphingolipids have been the focus of extensive research, and LC-MS/MS has become an essential tool in sphingolipid profiling. Although increased levels of glycosphingolipids have been reported in several sphingolipidoses, their relatively low sensitivity and specificity limit their utility as diagnostic biomarkers.[3] In contrast, lysosphingolipids (LysoSLs)—the N-deacylated derivatives of glycosphingolipids—have been found to accumulate markedly in the plasma and urine of patients with sphingolipidoses. These findings support their potential as sensitive and specific biomarkers for both diagnosis and therapeutic monitoring.[4]

Various forms of LysoSLs (LysoSLs) have been found to be selectively elevated in specific sphingolipidoses. For instance, significantly increased levels of globotriaosylsphingosine (LysoGb3) have been detected in both plasma and urine of male and female patients with FD.[5-7] In Krabbe disease, galactosylsphingosine (GalSph) is markedly elevated,[8,9] while glucosylsphingosine (GlcSph) shows a significant increase in GD.[3] Additionally, lysosphingomyelin (LysoSM), the N-deacylated derivative of sphingomyelin, has been reported to accumulate in patients with NPA, NPB, and NPC.[10,11]

The aim of this study was to establish and validate a robust analytical method for the simultaneous quantification of hexosylsphingosine (HexSph), LysoGb3, and LysoSM using LC-MS/MS. This method was optimized for use in clinical laboratories to support the diagnostic workflow for suspected sphingolipidoses and to monitor biochemical responses in patients receiving specific therapies, such as enzyme replacement therapy or substrate reduction therapy. The development of a multiplex assay for LysoSLs not only improves diagnostic efficiency but also facilitates the early detection and longitudinal assessment of disease activity, potentially leading to better patient outcomes. Our study introduces a locally optimized, rapid multiplex LC–MS/MS workflow for simultaneous quantification of LysoGb3, LysoSM, and HexSph with a 10-minute run time, which is shorter than that of comparable published methods.[12]

MATERIALS AND METHODS

Reagents and Chemicals

The following chemicals and reagents were used for LysoSL analyses: GlcSph (bovine buttermilk), N-omega-CD3-octadecanoyl-ceramide trihexoside (internal standard 1537; Matreya Chemicals), GalSph, LysoSM, LysoGb3, acetonitrile, methanol, acetone, chloroform, formic acid, and ultrapure water.

Sample Collection

Ethical approval was obtained from the Ethics Committee of Akdeniz University Faculty of Medicine (decision number: 373, dated: 30.05.2018). After obtaining informed consent, venous blood samples were collected into K2-EDTA tubes from 14 patients diagnosed with Fabry or GD and from 20 healthy adult volunteers at Akdeniz University Hospital. Plasma samples were separated and stored for analysis. Diagnoses were confirmed in all patients through demonstration of significant lysosomal enzyme deficiencies and/or mutation analysis.

Preparation of LysoSL Calibration Standards

Stock standard solutions were prepared by dissolving purified standards in a chloroform:methanol (2:1, v/v) mixture at the following concentrations: GlcSph, 0.5 mg/mL; LysoSM, 1 mg/mL; and LysoGb3, 0.1 mg/mL. GlcSph was used as the standard for HexSph. Working solutions at a concentration of 10 µmol/L for each analyte were prepared in the same solvent mixture and stored at -20 °C. These working solutions were diluted with methanol/acetone/water (45:45:10, v/v) to a final concentration of 10 nmol/L to prepare the precipitation solution containing the internal standard. A deuterium-labeled internal standard, N-omega-CD3-octadecanoyl-ceramide trihexoside (C18-CD3-Gb3), was used for quantification.

Calibration curves were constructed using six concentrations prepared by serial dilution of the stock solutions. The calibration ranges were 0-200 nmol/L for LysoGb3 and LysoSM, and 0-1000 nmol/L for HexSph. The accuracy and precision of the assay were evaluated using QC samples prepared at two concentration levels.

Sample Preparation

To 100 µL of plasma, calibrator, or QC sample, 500 µL of working precipitation solution was added. After vortexing for 30 seconds, the mixture was sonicated for 1 minute and subsequently centrifuged at 16,200 × g for 10 minutes. The clear supernatant was transferred to a new tube and evaporated under nitrogen. The dried residue was reconstituted in 100 µL of acetonitrile/water (1:1, v/v) containing 0.1% formic acid and centrifuged again at 16,200 × g for 10 minutes prior to LC-MS/MS analysis.

LC-MS/MS Method Optimization

Chromatographic separation of LysoGb3, HexSph, and LysoSM was achieved using a reverse-phase Raptor acid-resistant C18 column (2.1 × 100 mm, 2.7 µm particle size; Restek, USA). Because GlcSph and GalSph co-elute on this column, the two analytes were quantified together as HexSph (GlcSph + GalSph). Unlike most published studies focusing on a single analyte–disease pair, we provide a multiplexed approach applicable to multiple sphingolipidoses.

Mass spectrometric detection was performed on a UFLC-MS/MS system (LC-20 AD UFLC XR, Shimadzu 8040, Japan) equipped with a positive-mode electrospray ionization source. For each analyte, the precursor ions and optimized transitions were selected and monitored in multiple reaction monitoring mode. Detailed LC-MS/MS parameters are provided in Table 1.

Method Validation

The accuracy of the method was evaluated using quality control (QC) samples. Accuracy was calculated as the relative error (%), which was obtained by subtracting the nominal value from the mean measured value, dividing the difference by the nominal value, and multiplying by 100. Intra-day and inter-day precision were assessed by analyzing each standard in triplicate over consecutive days. Linearity was evaluated using six-point calibration curves for each biomarker. The limit of detection (LOD) and limit of quantification (LOQ) were determined for all analytes. Carryover effects were assessed by injecting blank samples after the highest calibration standard.

Table 1. Detailed LC-MS/MS parameters.

Parameter	Description
Mass spectrometer	Shimadzu 8040
Ionization mode	ESI, positive mode (+)
Column	Raptor ARC-18, 2.1 × 100 mm, 2.7 µm particle size
Column temperature	45 °C
Mobile phase A	H_2O + 0.1% FA
Mobile phase B	ACN + 0.1% FA
Gradient program (Pump B)	Time (min) %B 0–4 80 4–6 100 6–10 40
Flow rate	0.5 mL/min
Injection volume	2 µL
Total run time	10 minutes

H_2O 0.1% FA; water containing 0.1 percent FA, ACN 0.1% FA; acetonitrile containing 0.1 percent FA. ARC-18, acid-resistant C18; ESI, electrospray ionization; FA, formic acid.

Statistical Analysis

Statistical analyses were performed using SPSS version 20.0. Differences between groups were assessed using a two-tailed Student's t-test. A p-value ≤ 0.05 was considered statistically significant.

RESULTS

Chromatographic Analysis of LysoSLs

Chromatographic separation of LysoSLs was achieved with retention times of 1.57 minutes for LysoGb3, 1.72 minutes for LysoSM, and 1.98 minutes for HexSph. However, to ensure complete column elution and prevent carryover, the total run time was set to 10 minutes (Figure 1).

Linearity, Detection, and Quantification Limits

Repeated calibration curves were generated to assess linearity for LysoGb3, LysoSM, and HexSph, and the r^2 values were 0.995 for LysoSM, 0.982 for HexSph, and 0.961 for LysoGb3. A blank sample was injected after the highest calibration standard, and no carry-over was observed. The LOD and LOQ for LysoSLs were calculated from the mean and standard deviation of blank samples, which were run to obtain those statistics. The LOD and LOQ for LysoSLs were 0.012 and 0.036 nmol/L for LysoSM, 0.01 and 0.03 nmol/L for HexSph, and 7.18 and 21.54 nmol/L for LysoGb3, respectively (Table 2).

Precision and Accuracy

Precision and accuracy for each analyte were determined intraday (n = 5) and interday (n = 5). The % CV was below 20% for LysoSM and HexSph at all concentrations tested, whereas for LysoGb3 it was below 20% at 25 nmol/L and above.

LysoSL Levels in Healthy Controls and Lysosomal Disease (LD) Patients

Demographic characteristics of the study groups are summarized in Table 3. All Gaucher patients had Type 1 disease. Our study cohort consisted of seven male patients with the classic Fabry phenotype and three female patients with a stroke-associated Fabry phenotype. All patients were genetically confirmed. None of the patients were on enzyme replacement therapy at the time

of sampling. Plasma concentrations of LysoGb3, LysoSM, and HexSph in patients and controls are shown in Table 4.

Patients with GD exhibited significantly higher mean plasma levels of LysoSM and HexSph than those in healthy individuals. Although LysoGb3 levels were numerically higher in Fabry patients than in controls, the difference did not reach statistical significance ($p = 0.08$). The lack of statistical significance is likely due to the limited sample size (n=10) and the considerable

Table 2. Mass shifts and retention times of LysoSLs in LC-MS/MS.

Compound	Precursor ion (m/z)	Product ion (m/z)	Retention time (min)
LysoGb3	786.20	282.20	1.57
LysoSM	465.20	184.10	1.72
HexSph	462.20	282.30	1.98
LysoGb3-IS	843.20	264.30	1.40

Table 3. Demographic characteristics of patients and healthy controls.

Group	Controls	FD	GD
Sample size	20	10	4
Sex (M/F)	10/10	7/3	4/0
Age (mean, range)	37 (21–77)	37 (22–51)	40 (38–42)

Table 4. Plasma LysoSL levels in Gaucher and Fabry patients vs. healthy controls.

LysoSL	Group	Mean ± SEM (nmol/L)	p-value
LysoSM	Gaucher (n=4)	0.87 ± 0.28	0.001
	Control (n=20)	0.25 ± 0.02	
HexSph	Gaucher (n=4)	0.83 ± 0.39	0.001
	Control (n=20)	0.02 ± 0.002	
LysoGb3	Fabry (n=10)	35.63 ± 15.89	0.08
	Control (n=20)	10.03 ± 0.28	

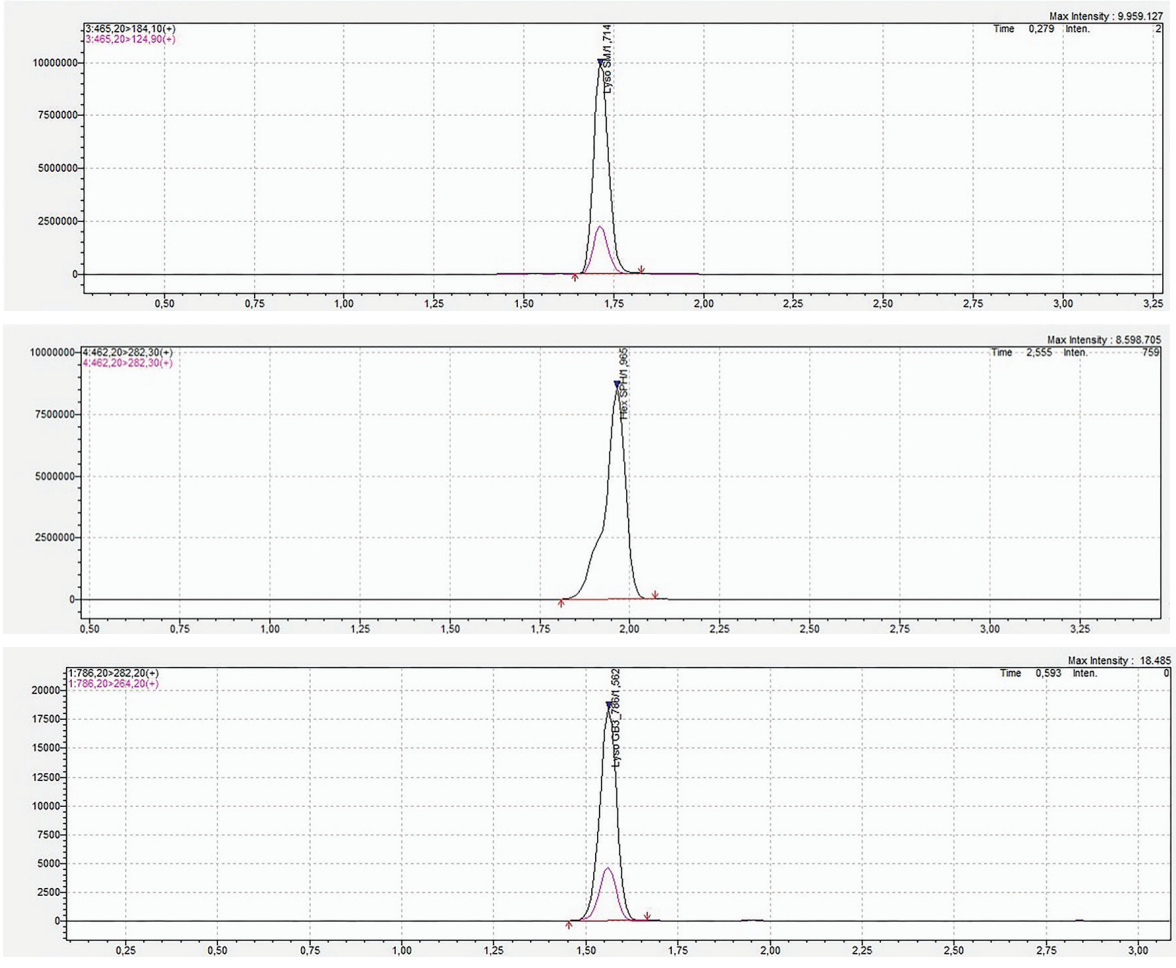


Figure 1. Chromatographic separation of LysoSLs with ARC-18 column in the 100 nmol/L calibrator (A. LysoSM 1.72, B. HexSph 1.98, C. LysoGb3 has an elution time (retention time) of 1.57 min.

variability between patients. In addition, differences in matrix and calibration, which affect absolute concentrations, may have masked numerical differences, even though they do exist.

DISCUSSION

LysoSLs have emerged as reliable and informative biomarkers for the diagnosis, prognosis, and therapeutic monitoring of sphingolipidoses, a group of inherited LSDs characterized by the accumulation of sphingolipid substrates due to enzyme deficiencies.[3,5] Numerous LC-MS/MS methods have been developed for the quantification of LysoSLs in various biological matrices, including plasma, urine, and dried blood spots.[6,9,11–15] However, a significant limitation of many previously published assays is their focus on a single analyte associated with a specific disease. While such approaches are effective for targeted diagnostics, they may fail to capture the broader metabolic alterations observed in LDs with overlapping or non-specific symptoms.

Recent studies have highlighted the value of multiplex panels that allow for the simultaneous measurement of multiple LysoSLs, suggesting that such panels can improve diagnostic yield, reduce turnaround time, and enhance cost-efficiency, particularly in high-throughput clinical settings.[14] The ability to evaluate multiple biomarkers from a single sample can also be particularly advantageous in early screening programs or when patient sample volume is limited. Moreover, multiplexing supports a more comprehensive understanding of disease pathology and may help differentiate between related disorders or phenotypic variants.

In this study, we developed and validated a rapid and accurate UFLC-MS/MS method for the simultaneous quantification of three key LysoSLs—HexSph (a combination of GlcSph and GalSph), LysoGb3, and LysoSM—in human plasma. The method is based on simple protein precipitation, avoiding the need for complex and time-consuming liquid–liquid extraction protocols. This streamlined sample preparation significantly reduces overall analysis time and enables high-throughput testing without compromising sensitivity or accuracy. The developed method is rapid, reproducible, and suitable for clinical laboratories. It simplifies sample preparation, reduces run time, and provides robust quantification.

Chromatographic separation was performed on a reversed-phase C18 column, which enabled efficient retention and resolution of LysoSLs. Due to the structural similarity between GlcSph and GalSph, these analytes were not resolved and were therefore reported collectively as HexSph. The use of a deuterated LysoGb3 internal standard ensured analytical robustness and reproducibility. The method demonstrated excellent linearity, precision, and accuracy, with detection and quantification limits comparable to or better than those reported in prior literature.

The analysis enabled the quantification of plasma LysoSL levels in healthy controls and in subjects with confirmed Gaucher and FD. Among Gaucher patients, LysoSM and HexSph were significantly elevated compared with controls, suggesting their relevance as disease-specific biomarkers. These findings are consistent with previous studies reporting elevated levels of LysoSM and GlcSph in GD, which is caused by β-glucocerebrosidase deficiency. In Fabry patients, plasma LysoGb3 levels were increased; however, this difference did not reach statistical significance, potentially owing to the limited sample size and the cross-sectional design of the study. Larger cohort studies may be needed to fully validate the diagnostic sensitivity and specificity of LysoGb3 in this population. During the study period (2018-2019), commercial control materials were not yet available in our laboratory.

Importantly, our method's short run time (10 minutes per sample) and compatibility with standard LC-MS/MS instrumentation make it well-suited for routine clinical application. The proposed panel could be expanded in future studies to include additional LysoSLs or disease-specific lipid species, thereby increasing its diagnostic utility. Furthermore, monitoring LysoSL levels over time may provide insights into disease progression and response to treatment, particularly in patients receiving enzyme replacement therapy or substrate reduction therapy.[16]

CONCLUSION

This study presents a robust, high-throughput UFLC-MS/MS method for the simultaneous quantification of clinically relevant LysoSLs in plasma. The approach holds promise for improving the efficiency and diagnostic accuracy of sphingolipidosis screening and may serve as a valuable tool in both clinical and research settings. Further validation in larger and more diverse patient populations is warranted to fully establish its diagnostic and prognostic utility.

Ethics

Ethics Committee Approval: Ethical approval was obtained from the Ethics Committee of Akdeniz University Faculty of Medicine (decision number: 373, dated: 30.05.2018).

Informed Consent: Informed consent was obtained from the parents of all patients included in this paper.

Footnotes

Authorship Contributions

Surgical and Medical Practices: H.A., E.S., Concept: H.A., Data Collection or Processing: H.A., B.K.E., N.Ö., Analysis or

Interpretation: H.A., E.S., Literature Search: H.A., A.E.B., B.K.E., Writing: H.A., A.E.B., B.K.E.

Conflict of Interest: The authors have no conflicts of interest to declare.

Financial Disclosure: This study was supported by Akdeniz University Scientific Research Projects Coordination Unit with project number TKA-2018-3847. The funding organization played no role in the study design; in the collection, analysis, and interpretation of data; in the writing of the report; or in the decision to submit the report for publication.

REFERENCES

1. Schulze H, Sandhoff K. Sphingolipids and lysosomal pathologies. Biochim Biophys Acta. 2014;1841(5):799-810. doi: 10.1016/j.bbalip.2013.10.015
2. Platt FM. Sphingolipid lysosomal storage disorders. Nature. 2014;510(7503):68-75. doi: 10.1038/nature13476
3. Dekker N, van Dussen L, Hollak CE, Overkleeft H, Scheij S, Ghauharali K, van Breemen MJ, Ferraz MJ, Groener JE, Maas M, Wijburg FA, Speijer D, Tylki-Szymanska A, Mistry PK, Boot RG, Aerts JM. Elevated plasma glucosylsphingosine in Gaucher disease: relation to phenotype, storage cell markers, and therapeutic response. Blood. 2011;118(16):e118-e127. doi: 10.1182/blood-2011-05-352971
4. Ferraz MJ, Kallemeijn WW, Mirzaian M, Herrera Moro D, Marques A, Wisse P, Boot RG, Willems LI, Overkleeft HS, Aerts JM. Gaucher disease and Fabry disease: New markers and insights in pathophysiology for two distinct glycosphingolipidoses. Biochim Biophys Acta. 2014;1841(5):811-825. doi: 10.1016/j.bbalip.2013.11.004
5. Aerts JM, Groener JE, Kuiper S, Donker-Koopman WE, Strijland A, Ottenhoff R, van Roomen C, Mirzaian M, Wijburg FA, Linthorst GE, Vedder AC, Rombach SM, Cox-Brinkman J, Somerharju P, Boot RG, Hollak CE, Brady RO, Poorthuis BJ. Elevated globotriaosylsphingosine is a hallmark of Fabry disease. Proc Natl Acad Sci U S A. 2008;105(8):2812-2817. doi: 10.1073/pnas.0712309105
6. Boutin M, Gagnon R, Lavoie P, Auray-Blais C. LC-MS/MS analysis of plasma lyso-Gb3 in Fabry disease. Clin Chim Acta. 2012;414:273-280. doi: 10.1016/j.cca.2012.09.026
7. Gold H, Mirzaian M, Dekker N, Joao Ferraz M, Lugtenburg J, Codée JD, van der Marel GA, Overkleeft HS, Linthorst GE, Groener JE, Aerts JM, Poorthuis BJ. Quantification of globotriaosylsphingosine in plasma and urine of Fabry patients by stable isotope ultraperformance liquid chromatography-tandem mass spectrometry. Clin Chem. 2013;59(3):547-556. doi: 10.1373/clinchem.2012.192138
8. Igisu H, Suzuki K. Analysis of galactosylsphingosine (psychosine) in the brain. J Lipid Res. 1984;25(9):1000-1006. doi: 10.1016/S0022-2275(20)37736-1
9. Chuang WL, Pacheco J, Zhang XK, Martin MM, Biski CK, Keutzer JM, Wenger DA, Caggana M, Orsini JJ Jr. Determination of psychosine concentration in dried blood spots from newborns that were identified via newborn screening to be at risk for Krabbe disease. Clin Chim Acta. 2013;419:73-76. doi: 10.1016/j.cca.2013.01.017
10. Chuang WL, Pacheco J, Cooper S, McGovern MM, Cox GF, Keutzer J, Zhang XK. Lyso-sphingomyelin is elevated in dried blood spots of Niemann-Pick B patients. Mol Genet Metab. 2014;111(2):209-211. doi: 10.1016/j.ymgme.2013.11.012
11. Welford RW, Garzotti M, Marques Lourenço C, Mengel E, Marquardt T, Reunert J, Amraoui Y, Kolb SA, Morand O, Groenen P. Plasma lysosphingomyelin demonstrates great potential as a diagnostic biomarker for Niemann-Pick disease type C in a retrospective study. PLoS One. 2014;9(12):e114669. doi: 10.1371/journal.pone.0114669
12. Polo G, Burlina AP, Kolamunnage TB, Zampieri M, Dionisi-Vici C, Strisciuglio P, Zaninotto M, Plebani M, Burlina AB. Diagnosis of sphingolipidoses: a new simultaneous measurement of lysosphingolipids by LC-MS/MS. Clin Chem Lab Med. 2017;55(3):403-414. doi: 10.1515/cclm-2016-0340
13. Auray-Blais C, Blais CM, Ramaswami U, Boutin M, Germain DP, Dyack S, Bodamer O, Pintos-Morell G, Clarke JT, Bichet DG, Warnock DG, Echevarria L, West ML, Lavoie P. Urinary biomarker investigation in children with Fabry disease using tandem mass spectrometry. Clin Chim Acta. 2015;438:195-204. doi: 10.1016/j.cca.2014.08.002
14. Ferraz MJ, Marques AR, Gaspar P, Mirzaian M, van Roomen C, Ottenhoff R, Alfonso P, Irún P, Giraldo P, Wisse P, Sá Miranda C, Overkleeft HS, Aerts JM. Lyso-glycosphingolipid abnormalities in different murine models of lysosomal storage disorders. Mol Genet Metab. 2016;117(2):186-193. doi: 10.1016/j.ymgme.2015.12.006
15. Mirzaian M, Wisse P, Ferraz MJ, Gold H, Donker-Koopman WE, Verhoek M, Overkleeft HS, Boot RG, Kramer G, Dekker N, Aerts JM. Mass spectrometric quantification of glucosylsphingosine in plasma and urine of type 1 Gaucher patients using an isotope standard. Blood Cells Mol Dis. 2015;54(4):307-314. doi: 10.1016/j.bcmd.2015.01.006
16. Smid BE, Ferraz MJ, Verhoek M, Mirzaian M, Wisse P, Overkleeft HS, Hollak CE, Aerts JM. Biochemical response to substrate reduction therapy versus enzyme replacement therapy in Gaucher disease type 1 patients. Orphanet J Rare Dis. 2016;11:28. doi: 10.1186/s13023-016-0413-3

ORIGINAL ARTICLE

DOI: 10.4274/imdn.galenos.2026.2025-12

Inherit Metab Disord Nutr 2026;2:7–12

Confirmation and Determination of Urinary Ethylmalonic Acid by Capillary Electrophoresis with Indirect UV Detection

Mehmet Şerif Cansever[1,2], Kağan Çalışgan[3], Ertuğrul Kıykım[3], Tanyel Zubarioğlu[3], Ayşe Çiğdem Aktuğlu Zeybek[1,3], Fatma Bedia Erim Berker[4]

[1]İstanbul University-Cerrahpaşa, Cerrahpaşa Faculty of Medicine, Research Laboratory of Metabolism, İstanbul, Türkiye
[2]İstanbul University-Cerrahpaşa, Vocational School of Health Services, Department of Medical Laboratory Techniques, İstanbul, Türkiye
[3]İstanbul University-Cerrahpaşa, Cerrahpaşa Faculty of Medicine, Department of Pediatric Nutrition and Metabolism, İstanbul, Türkiye
[4]İstanbul Technical University, Department of Chemistry, İstanbul, Türkiye

Abstract

Objectives: Ethylmalonic acid (EMA) is a key urinary biomarker of ethylmalonic encephalopathy (EE), but routine gas chromatography–mass spectrometry (GC–MS) is time- and resource-intensive. This study aimed to develop and validate a simple, rapid capillary electrophoresis (CE) method with indirect ultraviolet (UV) detection for the quantitative determination of EMA in urine.

Materials and Methods: A fused-silica capillary and a background electrolyte containing 5 mmol/L 2,6-pyridinedicarboxylic acid and 0.1 mmol/L cetyltrimethylammonium bromide (pH 5.74) were used. Separation was performed at 28 kV and monitored at 200 nm. Fresh human urine was diluted 1:20, filtered, and used to prepare matrix-matched calibrators (10–750 µmol/L). Linearity, precision, sensitivity, and accuracy were assessed according to International Council for Harmonisation validation guidelines, using spiked urine samples. Electropherograms from healthy control urine, EMA-spiked urine, and urine from a patient with EE illustrated the applicability.

Results: Under optimized conditions, EMA migrated at approximately 2.0 min with baseline resolution from endogenous components. Calibration was linear between 10 and 750 µmol/L (R^2 = 0.99920). Within-run precision, expressed as relative standard deviation (%), was 0.17% for migration time and 0.89% for corrected peak area, while between-day precision for peak area was 1.91%. The limits of detection and quantification were 11.78 and 39.3 µmol/L, respectively. Recovery in spiked urine ranged from 96 ± 2% to 98 ± 2%.

Conclusion: The CE–UV method enables rapid, reliable quantification of urinary EMA with minimal sample preparation. Its short analysis time and modest instrumentation requirements support its use for first-line screening and monitoring of EE, with GC–MS reserved for confirmatory analyses.

Keywords: Ethylmalonic Acid, Electrophoresis, Capillary, Urine, Biomarkers, Metabolism, Inborn Errors

INTRODUCTION

Ethylmalonic encephalopathy (EE) is an autosomal recessive mitochondrial disorder caused by pathogenic variants in the *ETHE1* gene.[1] Clinically, EE is characterized by developmental delay, relapsing petechiae, orthostatic acrocyanosis, and chronic diarrhea, with a heterogeneous phenotype that can vary widely among patients.[2] The prognosis is poor. Approximately half of affected children die before the age of two due to metabolic decompensation.[3] Biochemical findings typically include persistently elevated lactate and increased butyryl- and isovalerylcarnitine in blood, together with urinary excretion of ethylmalonic acid (EMA), methylsuccinic acid, butyrylglycine, and isovalerylglycine.[1] Combined treatment with coenzyme Q10, N-acetyl cysteine, and decontamination of bowel with metronidazole results in marked neurological improvement, reduction of acrocyanosis and petechial lesions, and disappearance of diarrhea, especially in early treatment.[4]

Address for Correspondence: Mehmet Şerif Cansever, İstanbul University-Cerrahpaşa, Cerrahpaşa Faculty of Medicine, Research Laboratory of Metabolism, İstanbul, Türkiye; İstanbul University-Cerrahpaşa, Vocational School of Health Services, Department of Medical Laboratory Techniques, İstanbul, Türkiye
E-mail: mehmet.cansever@iuc.edu.tr **ORCID ID:** orcid.org/0000-0003-3315-5124

Received: 23.12.2025 **Accepted:** 19.02.2026 **Epub:** 23.02.2026 **Publication Date:** 13.03.2026

Cite this article as: Cansever MŞ, Çalışgan K, Kıykım E, Zubarioğlu T, Aktuğlu Zeybek AÇ, Erim Berker FB. Confirmation and determination of urinary ethylmalonic acid by capillary electrophoresis with indirect UV detection. Inherit Metab Disord Nutr. 2026;2:7–12

Copyright© 2026 The Author(s). Published by Galenos Publishing House on behalf of Child Nutrition Metabolism Association.
This is an open access article under the Creative Commons AttributionNonCommercial 4.0 International (CC BY-NC 4.0) License.

For disorders like EE, in which urinary organic acid analysis is integral to diagnosis, gas chromatography–mass spectrometry (GC–MS) remains the reference method for comprehensive analysis.[5] However, capillary electrophoresis (CE) offers an accessible and operationally simple alternative for targeted analytes. It enables rapid separations with minimal sample preparation and instrument time.[6,7] Indirect ultraviolet (UV) detection by CE has previously been applied to biologically relevant short-chain organic acids, including EMA.[8] More recently, urinary EMA has also been determined using CE with capacitively coupled contactless conductivity detection (CE–C^4D), illustrating detector-dependent trade-offs between sensitivity and instrumentation requirements.[9] These attributes make CE an attractive option for clinical laboratories performing high-throughput screening and follow-up quantification.

The objective of this study was to develop an simple, rapid, and accurate CE method to determine EMA in urine.

MATERIALS AND METHODS

Materials

EMA, cetyltrimethylammonium bromide (CTAB), and 2,6-pyridinedicarboxylic acid (PDCA) were obtained from Sigma-Aldrich, Merck (Darmstadt, Germany), and Fluka (Buchs, Switzerland), respectively. Solutions were prepared with purified, deionized water (Elgacam C114, Elga, England filtration system).

Urine samples were prepared daily by diluting fresh human urine in purified water. The dilution ratio was 1/20. EMA stock solution was dissolved in purified water and stored at +4 °C. Solutions prepared daily were filtered before analysis using a microfilter with a 0.45-µm pore size. The background electrolyte (BGE) used for separations consisted of 5 mmol/L PDCA and 0.1 mmol/L CTAB, adjusted to pH 5.74.

Apparatus and Operating Condition

Agilent CE system (Germany) equipped with a diode-array detector was used for EMA seperations. Agilent ChemStation software was used for data processing. 75-µm i.d. fused-silica capillaries for the separation experiment were purchased from Agilent. The total lengths of the capillary and the detector were 57 cm and 49 cm, respectively. The separations were performed at 28 kV with a wavelength set at 200 nm in indirect-UV mode.

The new fused-silica capillary adjustment was performed by rinsing with 1 mol/L NaOH for 30 min, followed by purified water for 10 min. The capillary was rinsed with 0.1 mmol/L NaOH and water for 3 min each, and was buffered for 3 min on each working day. A three-min flush with buffer was performed between runs. Injections were administered at 5 × 10−3 MPa for 5 s.

pH measurements were performed using Metrohm 654 Digital pH Meter (Metrohm, Switzerland) equipped with a pH glass electrode. The Addition of CTAB provided a positively charged inner surface, slowing or reversing electroosmotic flow (EOF) toward the anode, so that anionic analytes co-migrated with the bulk flow under the applied field.

Sample Preparation

Fresh urine was diluted 1/20 (urine/water), mixed, and filtered (0.45 µm) immediately prior to analysis. The 1:20 dilution was selected to minimize urine matrix effects (e.g., high ionic strength or conductivity and viscosity), which can compromise peak shape, current stability, and the migration-time repeatability in CE, while still enabling reliable detection and quantification of EMA within the validated range. This sample-handling approach is consistent with prior CE methods for urinary organic acids, where urine is commonly analyzed after centrifugation, with dilution as needed; a 1:20 final dilution has been reported for urine matrices in CE–based organic acid profiling.[10] Matrix-matched calibrators and recovery samples were prepared by spiking aliquots of 1/20-diluted pooled urine with EMA at specified concentrations (see Sections 2.4–2.5).

Calibration and Linearity

Method validation was performed according to the International Council for Harmonisation (ICH) Q2 (R^2) guideline.[11] Linearity was evaluated in 1:20-diluted human urine over the range 10–750 µmol/L EMA using matrix-matched external calibration. Calibration points across this range were injected ($n \geq 3$ per level), and peak quantification was performed using corrected peak areas (A/t). The calibration model was fitted using ordinary least squares linear regression.

Precision

Within-run precision was assessed by six successive injections ($n = 6$) of a 50 µmol/L EMA standard in urine diluted 1:20; precision was expressed as relative standard deviation (RSD%) for migration time and the corrected peak area (A/t). Between-day precision was determined as RSD% of peak areas from measurements obtained on three different days ($n = 3$).

Sensitivity Limit of Detection/Limit of Quantification (LOD/LOQ)

The LOD was defined as the EMA concentration producing a signal with peak height three times the baseline noise ($S/N \approx 3$), and the LOQ as the concentration corresponding to $S/N \approx 10$.

Accuracy (Recovery)

Accuracy was assessed by recovery experiments in urine diluted 1/20 at three EMA concentrations (25, 50, and 100 µmol/L). Each level was measured six times ($n = 6$), and recoveries were calculated as (measured/added) × 100%.

Data Processing

Electropherograms were integrated using ChemStation. Quantification employed corrected peak areas (A/t) to minimize run-to-run variability associated with migration time shifts. Quality metrics (linearity, precision, recovery, LOD/LOQ) were summarized according to ICH-style analytical validation conventions.

RESULTS

Validation Results

Method performance characteristics are summarized in Table 1. Linearity was demonstrated over 10–750 µmol/L using matrix-matched calibration in 1:20-diluted urine; the regression equation was $y = 2.25045 \times 10^{-3} x + 1.59091 \times 10^{-2}$ with $R^2 = 0.99920$ (Figure 1). Within-run precision, expressed as RSD%, was 0.17 RSD% for migration time and 0.89 RSD% for the corrected peak area (A/t) (n = 6). Between-day precision for corrected peak area was 1.91% RSD (three different days).

Sensitivity, assessed using signal-to-noise criteria, yielded an LOD of 11.78 µmol/L and an LOQ of 39.3 µmol/L. Accuracy assessed by recovery experiments at 25, 50, and 100 µmol/L (n = 6 each) showed recoveries ranging from 96 ± 2% to 98 ± 2% (Table 1).

EMA Electropherograms and Urinary EMA Levels

Under the separation conditions described above, EMA migrated at approximately 2.0 min. Electropherograms of a healthy control urine sample, a control urine sample spiked with EMA, and a urine sample from a patient diagnosed with EE are shown in Figure 2A–C, respectively. In the healthy control urine (Figure 1), no distinct peak was observed at the EMA migration time, indicating that EMA < LOQ (39.3 µmol/L) under the applied conditions. In the matrix-matched spiked urine (Figure 2B), pooled urine (1:20 dilution) fortified with EMA at 50 µmol/L produced a well-defined peak at the same migration time, confirming the peak identity and demonstrating baseline resolution from endogenous components. In the patient sample (Figure 2C), a prominent peak at ≈ 2.0 min was detected and quantified as 78.4 µmol/L EMA in the analyzed (1:20 diluted) urine, which is above the LOQ. Because indirect UV detection yields negative peaks, electropherograms were displayed after polarity inversion to facilitate visualization and integration. Urinary EMA levels for the illustrative samples are summarized in Table 2.

Table 1. Validation values.

	Parameter	Result
Precision	Within-run precision (corrected peak area, A/t), RSD% (n = 6)	0.89
	Within-run precision (migration time), RSD% (n = 6)	0.17
	Between-day precision (corrected peak area, A/t), RSD% (n = 3 days)	1.91
Sensitivity	LOD (µmol/L)	11.78
	LOQ (µmol/L)	39.30
Accuracy (recovery)	EMA-spiked urine samples (25 µmol/L), recovery (%)	96 ± 2
	EMA-spiked urine samples (50 µmol/L), recovery (%)	96 ± 2
	EMA-spiked urine samples (100 µmol/L), recovery (%)	98 ± 2

EMA, ethylmalonic acid; LOD, limit of detection; LOQ, limit of quantification; RSD, relative standard deviation.

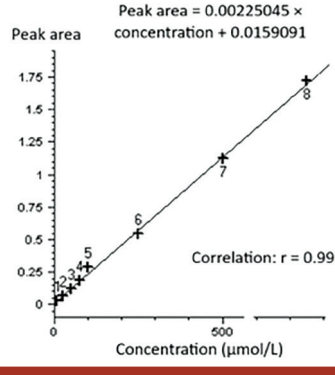


Figure 1. Calibration curve for EMA ethylmalonic acid.
EMA, ethylmalonic acid.

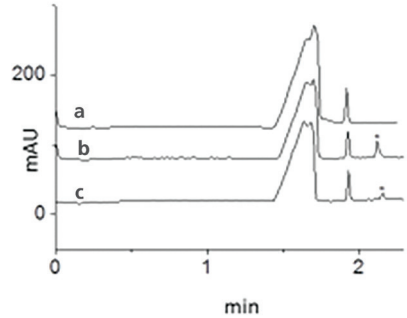


Figure 2. (a) Shows the electropherogram of healthy urine; (b) shows the electropherogram of a healthy urine spiked with EMA; (c) shows the electropherogram of a patient diagnosed with EE.
EE, ethylmalonic encephalopathy; EMA, ethylmalonic acid.

Table 2. Urinary EMA levels in illustrative human urine samples analyzed by CE–UV.

Sample (Figure 1)	Matrix/dilution	EMA status	Reported urinary EMA (µmol/L)	Interpretation
Healthy control	Urine, 1:20 diluted	Unspiked	<LOQ (39.3)*	Not quantifiable under conditions
Spiked control	Pooled urine, 1:20 diluted	Spiked	50	Peak identity confirmed at ≈ 2.0 min
EE patient	Urine, 1:20 diluted	Clinical sample	78.4	Quantifiable; above LOQ

*LOQ, 39.3 µmol/L. For the spiked sample, the concentration indicates the nominal added EMA level.

CE, capillary electrophoresis; EE, ethylmalonic encephalopathy; EMA, ethylmalonic acid; LOQ, limit of quantification; 2,6-pyridinedicarboxylic acid; UV, ultraviolet.

DISCUSSION

This study optimized a CE–UV method for the rapid quantification of urinary EMA. The method achieved a migration time of ~ 2 minutes in urine diluted 1:20, demonstrated excellent linearity across 10–750 µmol/L (r = 0.99920), exhibited tight intra- and interday precision, and showed high recovery. The LOD and LOQ were 11.78 and 39.3 µmol/L, respectively. EMA is a clinically significant urinary biomarker in EE and may be elevated in short-chain acyl-CoA dehydrogenase deficiency. Therefore, fast, reproducible first-line quantification of EMA has practical value for triage and monitoring.[1,12]

Traditionally, urine organic acid analysis is performed by GC–MS, which remains the confirmatory reference method. However, GC–MS requires derivatization and extraction as well as batch processing, which together extend turnaround times and increase resource use.[13] Faster preliminary results are clinically useful in disorders where EMA abnormalities inform acute and longitudinal management. This enables earlier decision-making while MS confirmation proceeds.[1] In this context, our CE–UV assay shortens the analytical step to minutes while maintaining the quantitative performance necessary for routine screening and monitoring. This enables a more efficient workflow in which cases that are clearly abnormal or ambiguous proceed to MS confirmation.[14]

The separation strategy employed in this study established principles for the separation of anionic analytes. Cationic surfactants, such as CTAB, dynamically modify the capillary wall, thereby reversing EOF. This promotes the rapid and reproducible migration of anions to the detector.[15,16] Because EMA lacks a strong native UV absorbance, indirect UV detection is appropriate. A Prior study has demonstrated indirect CE–UV of biologically relevant short-chain organic acids, including EMA, by using UV-absorbing co-ions and mobility matching.[8] The use of PDCA as the absorbing co-ion in the BGE during method implementations further supports robust indirect UV detection of carboxylic acids.[17] Our data expand upon existing literature by demonstrating the quantification of short-term EMA directly from minimally processed urine using a widely available UV/diode-array detector platform. Alternative CE implementations, such as CE–C^4D, have also achieved sensitive EMA detection, albeit with different detector trade-offs.[9]

Two methodological aspects merit emphasis. First, stable approximately 2-minute separations are achieved using low-level CTAB (0.1 mmol/L) with PDCA (5 mmol/L), a balanced EOF control, and indirect UV detection.[15] Second, our LOQ of 39.3 µmol/L is adequate for routine urine EMA screening within a reflex workflow, while CE–C^4D and MS methods achieve lower limits—an LOQ of ~ 3–4 µmol/L and an LOD of ~ 1 µmol/L—reflecting a trade-off between accessibility and sensitivity.[9] Given that EMA elevations in EE and related phenotypes are typically above normal, borderline results can be reflexed to MS for confirmation.[1]

From an interpretive standpoint, the method's analytical limitations should be considered when reporting results for healthy subjects and patients. In the healthy control (Figure 1), the absence of a distinct EMA peak at ≈ 2.0 min should be interpreted as EMA < LOQ (39.3 µmol/L) rather than complete absence. By contrast, the EE patient sample (Figure 1) showed an EMA concentration of 78.4 µmol/L in 1:20-diluted urine, which was readily quantifiable by CE–UV. Compared with indirect UV detection, CE–C^4D generally provides lower limits of detection for small ionic acids, which can improve interpretation of low-level or borderline EMA elevations (9).Therefore, samples near the LOQ or with strong clinical suspicion should be reflexed to CE–C^4D or MS-based confirmatory testing

This study has limitations. Indirect UV lacks the molecular specificity of MS; therefore, rare co-migrating matrix anions could interfere. This warrants orthogonal confirmation when measurements are near the LOQ or resolution is suboptimal. Also, the absolute concentrations in spot urine were reported without creatinine normalization. Laboratories that adopt this method should validate reporting in µmol/L with paired creatinine measurement or in mmol/mol creatinine, according to local practice standards. Finally, a head-to-head comparison against GC–MS and LC–MS in the same cohort was not performed to establish clinical concordance and decision thresholds for reflex testing.

In summary, we present a fast, precise, and accessible CE–UV assay for urinary EMA that can separate samples in approximately two minutes each with excellent linearity, low imprecision, and high recovery. In a reflex workflow, CE–UV can be used for same-

day screening. Samples with borderline concentrations can then be referred to GC–MS for confirmation or further analysis. This strategy could reduce turnaround time, allow GC–MS resources to focus on cases requiring greater specificity, reduce workload, and support longitudinal monitoring in EE.

CONCLUSION

A rapid and accessible CE–UV method for urinary EMA quantification was developed and validated. The assay provides an approximately 2-minute separation and demonstrates excellent linearity, low imprecision, and high recovery in urine diluted 1:20. This approach can support same-day screening and follow-up, with reflex MS confirmation recommended for borderline concentrations or when analytical specificity is required.

Ethics

Ethics Committee Approval: This study was approved by Clinical Research Ethical Committee of Cerrahpaşa Faculty of Medicine (approval number: E-29430533-604.01-01-273163, dated: 08.10.2015).

Informed Consent: All urine specimens were de-identified residual samples obtained during routine laboratory procedures, and no identifiable patient information was accessed. Therefore, the requirement for informed consent was waived by the Local Ethics Committee.

Footnotes

Authorship Contributions

Concept: M.Ş.C., E.K., T.Z., A.Ç.A.Z., F.B.E.B., Design: M.Ş.C., E.K., T.Z., A.Ç.A.Z., F.B.E.B., Data Collection or Processing: M.Ş.C., K.Ç., E.K., T.Z., A.Ç.A.Z., F.B.E.B., Analysis or Interpretation: M.Ş.C., K.Ç., E.K., T.Z., A.Ç.A.Z., F.B.E.B., Literature Search: M.Ş.C., K.Ç., E.K., T.Z., A.Ç.A.Z., F.B.E.B., Writing: M.Ş.C., K.Ç., E.K., T.Z., A.Ç.A.Z., F.B.E.B.

Conflict of Interest: One author of this article, Ertuğrul Kıykım, is a member of the editorial board of the Inherited Metabolic Disorders and Nutrition. However, he did not take part in any stage of the editorial decision of the manuscript. The editors who evaluated this manuscript are from different institutions. The other authors declared no conflict of interest.

Financial Disclosure: The authors declared that this study received no financial support.

REFERENCES

1. Di Meo I, Lamperti C, Tiranti V. Ethylmalonic Encephalopathy. In: Adam MP, Feldman J, Mirzaa GM, Pagon RA, Wallace SE, Amemiya A, editors. GeneReviews®. https://pubmed.ncbi.nlm.nih.gov/28933811/
2. Pigeon N, Campeau PM, Cyr D, Lemieux B, Clarke JTR. Clinical heterogeneity in ethylmalonic encephalopathy. J Child Neurol. 2009 Mar 16 [cited 2025 Oct 29]; Available from: https://journals.sagepub.com/doi/abs/10.1177/0883073808331359
3. Govindaraj P, Parayil Sankaran B, Nagappa M, Arvinda HR, Deepha S, Jessiena Ponmalar JN, Sinha S, Gayathri N, Taly AB. Child neurology: ethylmal encephalopathy. Neurology. 2020;94(12):e1336-1339. doi: 10.1212/WNL.0000000000009144
4. Viscomi C, Burlina AB, Dweikat I, Savoiardo M, Lamperti C, Hildebrandt T, Tiranti V, Zeviani M. Combined treatment with oral metronidazole and N-acetylcysteine is effective in ethylmalonic encephalopathy. Nat Med. 2010;16(8):869-871. doi: 10.1038/nm.2188
5. Kauna-Czaplińska J. Current applications of gas chromatography/mass spectrometry in the study of organic acids in urine. Crit Rev Anal Chem. 2011;41(2):114-123. doi: 10.1080/10408347.2011.555242
6. Cansever MŞ, Erim FB. Determination of urinary succinylacetone by capillary electrophoresis for the diagnosis of tyrosinemia type I. J Chromatogr B Analyt Technol Biomed Life Sci. 2005;818(2):309-311. doi: 10.1016/j.jchromb.2005.01.007
7. Ramautar R, Somsen GW, De Jong GJ. Direct sample injection for capillary electrophoretic determination of organic acids in cerebrospinal fluid. Anal Bioanal Chem. 2007;387(1):293-301. doi: 10.1007/s00216-006-0911-6
8. Chen H, Xu Y, Van Lente F, Ip MP. Indirect ultraviolet detection of biologically relevant organic acids by capillary electrophoresis. J Chromatogr B Biomed Appl. 1996;679(1–2):49-59. doi: 10.1016/0378-4347(96)00002-3
9. Özçelik S, Öztekin N, Kıykım E, Cansever MŞ, Aktuğlu-Zeybek AÇ. Capillary electrophoresis with capacitively coupled contactless conductivity detection for the determination of urinary ethylmalonic acid for the diagnosis of ethylmalonic aciduria. J Sep Sci. 2020;43(7):1365-1371. doi: 10.1002/jssc.201901044
10. García A, Barbas C, Aguilar R, Castro M. Capillary electrophoresis for rapid profiling of organic acidurias. Clin Chem. 1998 Sept;44(9):1905-1911. http://pubmed.ncbi.nlm.nih.gov/9732975/
11. International Council for Harmonisation of Technical Requirements for Pharmaceuticals for Human Use (ICH). ICH Q2(R^2) guideline on validation of analytical procedures – Step 5. Geneva: ICH; 2023. Available from: https://www.ich.org/page/quality-guidelines
12. Wolfe L, Jethva R, Oglesbee D, Vockley J. Short-Chain Acyl-CoA Dehydrogenase Deficiency. In: Adam MP, Feldman J, Mirzaa GM, Pagon RA, Wallace SE, Amemiya A, editors. GeneReviews®. https://pubmed.ncbi.nlm.nih.gov/21938826/
13. Gallagher RC, Pollard L, Scott AI, Huguenin S, Goodman S, Sun Q; ACMG Biochemical Genetics Subcommittee of the Laboratory Quality Assurance Committee. Laboratory analysis of organic acids, 2018 update: a technical standard of the American College of Medical Genetics and Genomics (ACMG). Genet Med. 2018;20(7):683-691. doi: 10.1038/gim.2018.45

14. Xiao Y, Sun C, Leung EKY. Urine organic acid testing in the clinical laboratory: the past, current, and future. Encyclopedia (Basel). 2025;5(3):153. doi: 10.3390/encyclopedia5030153

15. Lucy CA, Underhill RS. Characterization of the cationic surfactant induced reversal of electroosmotic flow in capillary electrophoresis. Anal Chem. 1996;68(2):300-305. doi: 10.1021/ac971476c

16. Diress AG, Lucy CA. Electroosmotic flow reversal for the determination of inorganic anions by capillary electrophoresis with methanol-water buffers. J Chromatogr A. 2004;1027(1–2):185-191. doi: 10.1016/j.chroma.2003.10.081

17. Chen Z, Tang C, Xu J. Non-suppressed conductivity and indirect UV detection of carboxylic acids in environmental samples by ion-exclusion chromatography using 2,6-pyridinedicarboxylic acidic eluent. J Chromatogr A. 1999;859(2):173-181. doi: 10.1016/s0021-9673(99)00885-7

CASE REPORT

DOI: 10.4274/imdn.galenos.2026.2025-11

Inherit Metab Disord Nutr 2026;2:13–15

A Novel *CLN1* Variant in a Turkish Patient with Infantile Neuronal Ceroid Lipofuscinoses

Tuğçe Aras Çöl[1], Seda Güneş[2], Elif İşler Soylu[1], Kağan Çalışgan[1], Hanım Babazade Aghakishili[1], Tanyel Zübarioğlu[1], Mehmet Şerif Cansever[1], Serdar Ceylaner[3], Ayşe Çiğdem Aktuğlu Zeybek[1]

[1]İstanbul University-Cerrahpaşa, Cerrahpaşa Faculty of Medicine, Department of Metabolism and Nutrition, İstanbul, Türkiye
[2]Harran University Faculty of Medicine, Department of Metabolism and Nutrition, Şanlıurfa, Türkiye
[3]Intergen Genetics and Rare Diseases Diagnosis Research and Application Center, Ankara, Türkiye

Abstract

The neuronal ceroid lipofuscinoses (NCLs) are a group of progressive neurodegenerative disorders characterised by abnormal accumulation of ceroid and lipofuscin in lysosomes and the cytoplasm. The progressive accumulation of ceroid and lipofuscin in the central nervous system leads to psychomotor retardation, vision loss, and epilepsy. NCLs are the most common neurodegenerative diseases of childhood, and a diagnosis of NCLs should be considered in individuals presenting with characteristic clinical symptoms and magnetic resonance imaging findings. A definitive diagnosis should be confirmed by an enzyme activity assay, skin biopsy or variant analysis. We present a case of infantile NCL with a novel variant.

Keywords: *CLN1*, Infantile neuronal ceroid lipofuscinoses, Novel variant

INTRODUCTION

The neuronal ceroid lipofuscinoses (NCLs) are a group of inherited, progressive neurodegenerative disorders that primarily affect children. They are among the most common neurodegenerative diseases of childhood. The age at which symptoms first appear can range from birth to adulthood. The main clinical symptoms are vision loss, dementia, loss of motor skills, epilepsy and, eventually, premature death.[1] NCLs are characterised by total brain atrophy and the abnormal accumulation of autofluorescent pigment in neuronal tissues.[2]

NCLs are classified both clinically and genetically. They are categorised by the age at which the disease manifests (congenital, infantile, late-infantile, juvenile, or adult) and by the defective gene. To date, fourteen different NCL forms have been described based on genetic analysis.[3] However, NCLs are a genetically heterogeneous group, and variants in the same gene can lead to different clinical courses.[4] A definitive diagnosis should be confirmed by both an enzyme activity assay and variant analysis. Here, we present a case of infantile NCL with a novel variant.

CASE REPORT

A two-year-old girl born to parents who were first-degree cousins presented to our clinic with restlessness. The prenatal, natal, and postnatal periods were uneventful, and she developed age-appropriate physical skills by one year of age. The patient had approximately 10–15 meaningful words at 12 months of age; however, her speech development did not progress further and subsequently regressed. She gradually lost previously acquired words and developed an articulation impairment. After the age of one year, her parents noticed a significant deterioration in her speech and other cognitive functions. The patient achieved independent walking at 13 months of age; however, her gait became ataxic after one year of age and progressively

Address for Correspondence: Tuğçe Aras Çöl, İstanbul University-Cerrahpaşa, Cerrahpaşa Faculty of Medicine, Department of Metabolism and Nutrition, İstanbul, Türkiye
E-mail: tugce.col@iuc.edu.tr **ORCID ID:** orcid.org/0009-0001-5781-1168

Received: 22.12.2025 **Accepted:** 24.03.2026 **Epub:** 12.03.2026 **Publication Date:** 09.06.2026

Cite this article as: Aras Çöl T, Güneş S, İşler Soylu E, Çalışgan K, Babazade Aghakishili H, Zübarioğlu T, Cansever MŞ, Ceylaner S, Aktuğlu Zeybek AÇ. A novel *CLN1* variant in a Turkish patient with infantile neuronal ceroid lipofuscinoses. Inherit Metab Disord Nutr. 2026;2:13–15

Copyright© 2026 The Author. Published by Galenos Publishing House on behalf of Child Nutrition Metabolism Association.
This is an open access article under the Creative Commons AttributionNonCommercial 4.0 International (CC BY-NC 4.0) License.

deteriorated, such that by 18 months she had completely lost her ability to walk. She developed myoclonic jerks, both spontaneous and stimulus-sensitive. There was no history of prolonged epileptic seizures or status epilepticus.

On physical examination, she was conscious and had significant hypotonia in her trunk and severe hypertonia in her limbs. Her deep tendon reflexes were increased. No visual tracking response was observed during the examination. Fundoscopic examination could not be performed at the time of evaluation; therefore, retinal findings could not be assessed. Examinations of the cardiac and respiratory systems were normal. There was no evidence of organomegaly. Inborn errors of metabolism, such as congenital defects of glycosylation, leukodystrophies, mitochondrial cytopathies, and NCL, were considered in the differential diagnosis. The complete blood count and biochemical parameters were within normal limits. Metabolic screening tests, such as Tandem MS and urinary organic acid analysis, revealed no pathological findings; however, nonspecific changes were observed in quantitative blood amino acid levels. Magnetic resonance imaging (MRI) of the brain revealed diffuse cerebral atrophy and corpus callosum agenesis. A skin biopsy revealed the presence of loose, membrane-bound granular osmiophilic deposits in sweat gland epithelial cells, blood vessel smooth muscle cells, endothelial cells, and fibroblasts. Examination by electron microscopy revealed buffy coat lymphocytes, which, together with the storage inclusions seen in the skin biopsy, were typical of the classic form of infantile NCL.

CLN1 gene sequencing was performed using the MiSeq next-generation sequencing platform (Illumina, San Diego, California, USA) according the manufacturer's instructions. The sequences were then aligned to the hg19 genome using the MiSeq Reporter software (Illumina Inc.). The data were visualised using IGV 2.3 (Broad Institute). A homozygous p.P238Cfs*56 (c.712_713delCC) variant was identified. This frameshift variant is predicted to result in a premature stop codon, leading to a truncated and likely non-functional protein. According to the American College of Medical Genetics and Genomics/Association for Molecular Pathology guidelines, the variant was classified as likely pathogenic. The frameshift nature supports the PVS1 criterion, and its absence from population databases and an in-house cohort of approximately 300 Turkish exome datasets supports PM2. In addition, *in silico* prediction tools provided supporting evidence, although conflicting results were also noted.The variant was further evaluated using standard bioinformatics pipelines in an in-house exome sequencing database comprising approximately 300 individuals of Turkish origin and was not detected in this cohort. Enzyme analysis was requested; however, the results were not available at the time of writing. Segregation analysis in the family was requested; however, the results were not available at the time of writing.

DISCUSSION

Here, we present a Turkish patient with infantile NCL carrying a novel *CLN1* variant. To date, fourteen different NCLs have been described, although some individuals with NCL were described as having a classical disease presentation despite no mutation being detected in the *NCL* gene.[1] *CLN1*, *CLN2*, *CLN10*, and *CLN13* are caused by defects in *lysosomal enzymes*, while *CLN3*, *CLN6*, *CLN7*, and *CLN8* are caused by defects in transmembrane proteins. *CLN12* and *CLN14*, on the other hand, are caused by mutations in the ATPase and potassium channel genes, respectively.[1,5,6] A newly described *CLN4* gene plays an important role in putative synaptic functions.[7]

Infantile NCL is caused by defects in palmitoyl-protein thioesterase-1 (PPT-1). PPT-1 cleaves long-chain fatty acid moieties from cysteine residues on a multitude of protein targets.[8]

NCLs present with similar clinical manifestations, including cognitive decline, motor impairment, myoclonus, seizures, deteriorating visual acuity, and other visual impairments. Although there are no specific laboratory tests available for NCL, MRI findings such as diffuse atrophy, cerebral atrophy, cerebellar atrophy and thalamic T2-weighted hypointensity, as well as diffuse T2-weighted hyperintensity in the periventricular area and centrum semiovale, can aid the differential diagnosis of NCL.[1,2]

In our patient, agenesis of the corpus callosum was also observed on MRI. This finding is not commonly reported in classical infantile *CLN1*-related NCL and may represent either an additional feature or a coincidental anomaly.

In infantile NCL, a previously healthy, normally developing child begins to lose developmental milestones. Additional symptoms include myoclonus, visual impairment and refractory seizures. Infantile NCL is a rapidly progressive lysosomal storage disorder, with patients experiencing fulminant brain atrophy and progressive microcephaly.[8] Electron microscopy of affected tissues demonstrates the accumulation of granular osmiophilic dense bodies. Our patient exhibits the same clinical features as those reported in the literature.[2] Although the identified variant is compatible with the clinical and pathological findings, the absence of enzyme activity analysis, segregation data, and fundoscopic examination is an important limitation. Biochemical and functional validation would further strengthen the diagnostic accuracy and interpretation of the variant.

To date, 64 pathogenic variants have been identified in the *CLN1* gene. The novel variant detected in our patient expands the mutational spectrum of *CLN1*-related disease. NCLs may present in congenital, infantile, late-infantile, juvenile, or adult

forms. However, this variant did not produce any additional or atypical phenotypic features. The patient exhibited findings fully consistent with the classical infantile form, indicating that the newly identified genotype does not appear to alter the expected clinical presentation. Further cases and functional studies will be necessary to confirm its pathogenicity and to determine whether this variant has any subtle effects on disease progression.

CONCLUSION

We present the case of a Turkish patient with classic infantile NCL who carries a novel *CLN1* variant. While this variant expands the known *CLN1* mutational spectrum, it does not appear to alter the expected clinical phenotype. The patient's symptoms were fully consistent with the classical infantile form. Further cases and functional studies are required to confirm the pathogenicity of this variant.

Ethics

Informed Consent: Informed consent was obtained from the parents of all patients included in this paper.

Footnotes

Authorship Contributions

Concept: T.A.Ç., S.G., Design: T.A.Ç., S.G., E.İ.Ş., A.Ç.A.Z., Data Collection or Processing: T.A.Ç., S.G., E.İ.Ş., K.Ç., T.Z., M.Ş.C., S.C., A.Ç.A.Z., Analysis or Interpretation: T.A.Ç., S.G., K.Ç., H.B.A., T.Z., M.Ş.C., S.C., A.Ç.A.Z., Literature Search: T.A.Ç., S.G., H.B.A., T.Z., S.C., A.Ç.A.Z., Writing: T.A.Ç., S.G.

Conflict of Interest: The author(s) have no conflicts of interest to declare.

Financial Disclosure: The author(s) declared that this study received no financial support.

REFERENCES

1. Schulz A, Kohlschütter A, Mink J, Simonati A, Williams R. NCL diseases: Clinical perspectives. Biochim Biophys Acta. 2013;1832(11):1801-1806. doi: 10.1016/j.bbadis.2013.04.008
2. Bennett MJ, Rakheja D. The neuronal ceroid-lipofuscinoses. Dev Disabil Res Rev. 2013;17(3):254-259. doi: 10.1002/ddrr.1118
3. Williams RE, Mole SE. New nomenclature and classification scheme for the neuronal ceroid lipofuscinoses. Neurology. 2012;79(2):183-191. doi: 10.1212/WNL.0b013e31825f0547
4. Kousi M, Lehesjoki AE, Mole SE. Update of the mutation spectrum and clinical correlations of over 360 mutations in eight genes that underlie the neuronal ceroid lipofuscinoses. Hum Mutat. 2012;33(1):42-63. doi: 10.1002/humu.21624
5. Bras J, Verloes A, Schneider SA, Mole SE, Guerreiro RJ. Mutation of the parkinsonism gene *ATP13A2* causes neuronal ceroid-lipofuscinosis. Hum Mol Genet. 2012;21(12):2646-2650. doi: 10.1093/hmg/dds089
6. Staropoli JF, Karaa A, Lim ET, Kirby A, Elbalalesy N, Romansky SG, Leydiker KB, Coppel SH, Barone R, Xin W, MacDonald ME, Abdenur JE, Daly MJ, Sims KB, Cotman SL. A homozygous mutation in *KCTD7* links neuronal ceroid lipofuscinosis to the ubiquitin-proteasome system. Am J Hum Genet. 2012;91(1):202-208. doi: 10.1016/j.ajhg.2012.05.023
7. Arsov T, Smith KR, Damiano J, Franceschetti S, Canafoglia L, Bromhead CJ, Andermann E, Vears DF, Cossette P, Rajagopalan S, McDougall A, Sofia V, Farrell M, Aguglia U, Zini A, Meletti S, Morbin M, Mullen S, Andermann F, Mole SE, Bahlo M, Berkovic SF. Kufs disease, the major adult form of neuronal ceroid lipofuscinosis, caused by mutations in *CLN6*. Am J Hum Genet. 2011;88(5):566-573. doi: 10.1016/j.ajhg.2011.04.004
8. Vesa J, Hellsten E, Verkruyse LA, Camp LA, Rapola J, Santavuori P, Hofmann SL, Peltonen L. Mutations in the palmitoyl protein thioesterase gene causing infantile neuronal ceroid lipofuscinosis. Nature. 1995;376(6541):584-587. doi: 10.1038/376584a0

REVIEW

DOI: 10.4274/imdn.galenos.2026.2025-13
Inherit Metab Disord Nutr 2026;2:16–24

A Brief Overview of Fatty Acid Oxidation Disorders

Mehmet Cihan Balcı

İstanbul University Faculty of Medicine, Department of Nutrition and Metabolism, İstanbul, Türkiye

Abstract

A number of genetic disorders affecting every stage of fatty acid oxidation (FAO) have been identified. The most common manifestations are fasting-induced hypoglycemia and, less commonly, life-threatening coma. The research findings indicate chronic cardiomyopathy and muscle weakness. Less frequently, evidence of rhabdomyolysis is observed. The initial symptoms may manifest at various stages, ranging from the neonatal period to adulthood. The diagnosis of this condition is facilitated by detecting elevated levels of abnormal acylcarnitines, which can be measured by tandem mass spectrometry. During periods of acute illness, initiating intravenous fluid therapy containing dextrose is recommended to suppress lipolysis. In long-term treatment, the most significant aspect is the prevention of prolonged fasting. This review aims to provide information on the clinical findings, diagnosis, and treatment methods of FAO disorders.

Keywords: Fatty acid oxidation, Reye-like syndrome, Hypoketotic hypoglycemia, Cardiomyopathy, Rhabdomyolysis

INTRODUCTION

All cells, with the exception of adult erythrocytes, use mitochondrial fatty acid oxidation (FAO) as the primary mechanism for the breakdown of long-chain fatty acids.[1] The mechanism of FAO was identified by German chemist Georg Franz Knoop in the 1900s.[2] His seminal research on odd- and even-chain ω-phenyl fatty acids demonstrated that fatty acid metabolism proceeded via removal of two-carbon units sequentially. In addition to promoting oxidative phosphorylation and the tricarboxylic acid (TCA) cycle, FAO increases the production of ketone bodies in the liver. This pathway is made up of 25 enzymes and specific transport proteins.[3] Furthermore, the FAO has been found to play a significant role in the pathophysiology of common disorders such as insulin resistance, diabetes, obesity, kidney fibrosis and heart failure.[2]

CLINICAL MANIFESTATIONS

Numerous clinical diseases are caused by disorders of FAO. Patients may exhibit completely diverse symptoms even if they have the same mutation.[4] Hypoketotic hypoglycemia during catabolic states such as illness, fever, fasting, and exercise may be a clinical sign in patients with FAO disorders (FAODs). Hypoketotic hypoglycemia can progress to Reye-like syndrome, which may lead to coma or death. Carnitine transporter deficiency (CTD), very long-chain acyl-CoA dehydrogenase (VLCAD), trifunctional protein (TFP), long-chain hydroxyacyl-CoA dehydrogenase (LCHAD), carnitine acyl-carnitine translocase (CACT), and carnitine palmitoyltransferase-II (CPT-II) deficiencies may manifest as hypertrophic or dilated cardiomyopathy.[5,6] Although there have been documented exceptions to this trend, patients with CPT-IA and medium-chain acyl-CoA dehydrogenase (MCAD) deficiencies typically do not have cardiomyopathy.[5-7] Patients with FAOD disorders may also present with arrhythmias and conduction deficits, but they often do not have cardiomyopathy.[5,6] The presence of these symptoms in CTD, CPT-IA, and MCAD deficiencies (MCADDs) is also controversial.[6]

Furthermore, skeletal myopathy, which is characterized by rhabdomyolysis, myalgia, and muscle weakness, may manifest or develop in patients with an FAOD.[5,6] These symptoms are the most common in patients who present at a later age. Moderate lipid accumulation may be seen in muscle biopsies, primarily in type 1 fibers.[8] VLCAD-deficient patients had proximal myopathy

Address for Correspondence: Mehmet Cihan Balcı, İstanbul University Faculty of Medicine, Department of Nutrition and Metabolism, İstanbul, Türkiye
E-mail: mcbalci@istanbul.edu.tr **ORCID ID:** orcid.org/0000-0002-3384-8679

Received: 03.01.2026 **Accepted:** 24.03.2026 **Epub:** 12.03.2026 **Publication Date:** 22.05.2026

Cite this article as: Balcı MC. A brief overview of fatty acid oxidation disorders. Inherit Metab Disord Nutr. 2026;2:16–24

Copyright© 2026 The Author. Published by Galenos Publishing House on behalf of Child Nutrition Metabolism Association.
This is an open access article under the Creative Commons AttributionNonCommercial 4.0 International (CC BY-NC 4.0) License.

whereas similar findings appeared in distal muscle groups in patients with LCHAD deficiency.[2]

Hepatomegaly likely reflects fatty liver.[6] Hepatic steatosis is primarily associated with MCADD, VLCAD deficiency (VLCADD), LCHAD/mitochondrial TFP deficiency, and multiple acyl-CoA dehydrogenase deficiency (MADD). Lipid accumulation in the liver results from inhibition of mitochondrial β-oxidation, thereby preventing hepatocytes from adequately using fatty acids as fuel during fasting, illness, or catabolic stress. Fatty acids that should be oxidized are instead re-esterified into triglycerides and retained in hepatocytes. Patients with LCHAD and MTP deficiencies may experience retinopathy and polyneuropathy (peripheral neuropathy).[9,10]

Hepatic, cardiac, and skeletal muscle signs and symptoms of early-onset multisystem failure are particularly common in long chain FAOD.[11] The heart has a continuously high energy demand to sustain contractile function. To secure continuous ATP production, the heart is a metabolic "omnivore" that can use many different substrates, depending on their availability.[12] FAO, however, is the preferred pathway for energy production in the heart, with more than half of ATP production derived from fatty acids. In contrast, the prenatal heart relies on glucose and lactate, but in the immediate postnatal period, when dietary fat is abundant, the heart switches to FAO as a source of energy.[13]

FAO is also crucial for ATP production in muscle; in particular, during exercise, FAO increases from rest to low-intensity exercise but does not increase further as exercise intensity increases. This pattern is in contrast to that seen for glucose and glycogen utilization, which always increase with exercise intensity. The sources of fatty acids also differ depending on the exercise intensity, with the contribution of plasma free fatty acids increasing with exercise intensity.[14]

In some patients, renal tubular disease may also be evident. Failure to supply the brain with glucose or ketones leads to neurological symptoms. Neonatal presentations usually feature undetectable protein expression or enzyme activity and are strongly associated with the severity of the mutation.[15]

The major manifestations of the late-onset forms of these disorders usually involve skeletal muscle or the heart. In these cases, residual enzyme activity and ketogenesis appear sufficient to preserve the liver and protect the brain from major involvement. Many patients with later-onset disease do not exhibit severe fasting intolerance but have exercise-induced rhabdomyolysis. In all long-chain FAOD that exhibit rhabdomyolysis, release of myoglobin may result in glomerular injury and acute renal failure.[11]

Many individuals are compound heterozygotes for a severe and a mild mutation, and intermediate forms of these long-chain FAODs exist. During fasting, these individuals are at risk of metabolic decompensation, hepatic failure, and potentially life-threatening hypertrophic cardiomyopathy. Additionally, some patients experience skeletal myopathy and are susceptible to acute muscle complaints, such as rhabdomyolysis, while under stress.[9,15,16]

Although the precise mechanisms causing heterogeneous presentations are still not completely known, as with many other enzyme deficiencies, the amount of residual activity of the enzyme is thought to define the clinical phenotype.[17] In addition to residual enzyme activity, other genetic and environmental factors have been found to be significant in the manifestation of disease. Heterogeneous clinical presentations within the same family provide particular evidence for this.[18] The marked intrafamilial phenotypic variability observed in FAODs suggests that the clinical course cannot be explained solely by the underlying pathogenic genotype. Even among relatives carrying the same disease-causing variant, presentations may range from severe neonatal or infantile disease to relatively mild, late-onset, or even apparently asymptomatic forms. This variability supports the concept that additional factors, including modifier genes, epigenetic mechanisms, residual enzyme activity, and environmental triggers such as fasting, intercurrent illness, dietary habits, and metabolic stress, contribute substantially to disease expression.

Carnitine Transporter Deficiency

Early childhood onset cardiomyopathy, with or without weakness and hypotonia, recurrent hypoglycemic hypoketotic seizures and/or coma, failure to thrive, and exceptionally low plasma and tissue carnitine concentrations are the hallmarks of CTD, a potentially fatal autosomal recessive disorder.[19] This condition exhibits phenotypic diversity; many patients develop symptomatic cardiomyopathy or recurrent hypoketotic hypoglycemia (Reye-like episodes) in early years of life.[4] Muscle hypotonia, modest developmental delay, failure to thrive, delayed walking, and poor growth are symptoms that newborns may initially exhibit. Some patients may have isolated cardiomyopathy, which can present with sudden death later in childhood. Within the same pedigree, both a symptomatic and symptomatic individuals have been reported.[18] Evidence suggests that compared to those who appear clinically, asymptomatic patients typically have slightly higher residual activity.[20] It is suggested carriers of a single *OCTN2* mutation may be susceptible to clinical illness if they experience enough stress.[19]

Carnitine Palmitoyltransferase-IA Deficiency

Related carnitine acyltransferases are encoded by 3 genes in the human genome. The liver isoform of CPT-I is encoded by *CPT-IA*, muscle-type CPT-I is encoded by CPT-IB, and CPT-IC encodes brain isoform.[21] The liver, kidney, lung, spleen, gut, pancreas, ovary, and fibroblasts all express CPT-IA isoform.[4]

The hepatic (and renal) CPT-IA deficiency is currently the sole known human CPT-I defect.[11] Patients with CPT-IA deficiency typically exhibit recurrent episodes of fasting-induced hepatic failure (Reye-like hepatic encephalopathy) with hypoketotic hypoglycemia, metabolic acidosis with elevated transaminases, hepatomegaly, hepatosteatosis, and mild to moderate hyperammonemia in infancy, reflecting the tissue localization of this isoform of CPT-IA.[11] Hypoglycemia stems from increased glucose utilization due to the inability to produce ketone bodies, and from decreased gluconeogenic capacity because of the absence of acetyl-CoA produced by FAO, a crucial activator of gluconeogenesis. The expression of CPT-IA in the renal tubular epithelium, which depends on FAO to sustain the high energy transport mechanisms, explains why renal tubular acidosis during catabolic periods has also been documented in a number of patients.[4]

Neonates have been documented to exhibit a variety of cardiac abnormalities, such as tachycardia, bradycardia, arrhythmias, right bundle branch block, and abrupt cardiac arrest.[4] One possible explanation is the expression of CPT-IA in the fetal heart, which persists until the neonatal stage.[22] Although hyperlipidemia is uncommon in other FAOD, hyperlipidemia with elevated triglycerides and/or cholesterol might be an additional feature of CPT-IA deficiency.[23] Hepatic VLDL production may be particularly favored by blockade of the outer mitochondrial membrane, leading to hyperlipidemia.

Carnitine Palmitoyltransferase-II Deficiency

There is one widely expressed isoform of the CPT-II enzyme.[4] There are three phenotypes of CPT-II deficiency: a lethal neonatal-onset form with congenital anomalies, a severe neonatal hepatocardiomuscular form, and a mild myopathic adult form.[4] Non-ketotic hypoglycemia, liver disease, hypotonia, cardiomyopathy, and congenital anomalies are the hallmarks of the fatal newborn phenotype.[24] The infantile form, whether there is cardiac disease or not, manifests as periods of decompensation with liver and skeletal muscle involvement, mainly as non-ketotic hypoglycemia caused by fasting and/or concurrent infection.[25] After childhood, cardiac symptoms are uncommon.[2]

About 50% of myopathic diseases are caused by the prevalent S113L mutation.[4] Because the frequent and high residual activity S113L mutation, causes the production of a thermolabile enzyme, the enzyme activity is further decreased by protein degradation during intense exercise when muscle temperature rises, aggravating the injury to the muscles.[4] The S113L variant, particularly in the homozygous state, is typically associated with the late-onset muscular form rather than with the severe neonatal or infantile forms. For infantile type CPT-II deficiency, there is no reliable genotype–phenotype correlation exists.[17]

Carnitine Acyl-Carnitine Translocase Deficiency

CACT deficiency causes heterogenous clinical phenotype.[26] Attenuated cases may manifest in the first few months of life, but severe neonatal-onset disease is most common, with symptoms emerging within two days of delivery.[26] Early-onset illness is characterized by hyperammonemia, cardiac arrhythmias, and an increased incidence of cardiac arrest. Clinical manifestations also include poor feeding, lethargy, hypoketotic hypoglycemia, hypotonia, transaminitis, liver dysfunction with hepatomegaly, and rhabdomyolysis. Cases of univentricular or biventricular hypertrophic cardiomyopathy, ranging from mild to severe, may improve with proper nutritional and medical interventions. Arrhythmia, especially ventricular tachycardia, is the most prominent cardiac manifestation during the neonatal period. This is followed by various tachyarrhythmias and bradyarrhythmias. Individuals with the early-onset form of the disease typically present with brain damage due to hyperammonemia. Patients with later-onset disease have milder symptoms and are less likely to experience recurrent hyperammonemia, leading to better developmental outcomes. Typically, carnitine levels are quite low (<5 μM).[2] In the plasma acylcarnitine profile, long-chain acylcarnitines are significantly elevated, whereas free carnitine levels are significantly reduced. Excess unsaturated species in urine organic acids can indicate severe dicarboxylic aciduria.[27] Differential diagnosis with genetic testing is necessary as this abnormal profile cannot be distinguished from that of neonatal CPT-2 deficiency.[27]

Very Long-chain Acyl-CoA Dehydrogenase Deficiency

The first rate-limiting stage of mitochondrial long-chain FAO is catalyzed by VLCAD.[11] Like other FAO enzymes, human VLCAD is highly active in the heart, liver, and skeletal muscle.[28] VLCADD is the most prevalent long-chain FAOD in the majority of populations.[29] The three main phenotypes of VLCADD are a late onset myopathic form, a milder childhood form that typically presents with hypoketotic hypoglycemia, but frequently has exercise intolerance and rhabdomyolysis as a significant feature, especially in older children and young adults.[4] A severe infantile phenotype manifests early in life with hypoglycemia, hepatic dysfunction, acidosis, and cardiomyopathy. Within the first few months, 75% of patients who survive early onset symptoms succumb to death.[30] Lower incidences of cardiomyopathy and hypoketotic hypoglycemia are features of childhood-onset

VLCADD, which is milder than early-onset. There has also been evidence of an association to rhabdomyolytic episodes in later childhood.[31]

Muscle pain and stiffness driven by exercise, fasting, temperature extremes, and occasionally infection are the hallmarks of the late-onset myopathic variants of both CPT-II and VLCADD.[4] Although about 20% of individuals will exhibit some lipid accumulation, muscle biopsies are often normal. When combined, these two conditions are the most prevalent inherited metabolic causes of rhabdomyolysis and myalgia in both adults and children.

Numerous *ACADVL* mutations have been identified, the most prevalent of which is c.848T>C.[32] The V243A mutation in the *VLCAD* gene has been identified in a large percentage of asymptomatic patients since newborn screening was implemented.[17] Which individuals, if any, may remain asymptomatic is unknown. There has also been evidence of a relationship between residual activity and clinical phenotype for VLCADD, with residual activities >10% indicating a milder phenotype.[33]

Long-Chain Hydroxyacyl-CoA Dehydrogenase Deficiency and Trifunctional Protein Deficiency

Isolated LCHADD is more common than TFP deficiency in relation to TFP functions.[4] Patients with TFP deficiency display a broad range of clinical symptoms, from mild to severe infantile presentation with hepatic indications to severe newborn manifestations such as cardiomyopathy and mortality.[18] Irreversible peripheral neuropathy and retinopathy presenting in TFP and LCHADD, have not been documented in any of the other long-chain FAOD.[17] Peripheral neuropathy develops in up to 80% of TFP deficient cases during long-term follow-up, according to various studies,[9,34] whereas in LCHADD, it is reported to occur only in 5–10% of cases.[35] In comparison, only 5–13% of patients with TFP deficiency and 30% to >50% of LCHADD patients are known to experience retinopathy.[9,34] These diseases typically manifest as episodic rhabdomyolysis during physical activity, illness, or fasting, however this may not show up for years following the initial neurological manifestation.[34,36] It has been suggested that the particular toxicity of the 3-hydroxacyl metabolites is the cause of the neuropathy and rhabdomyolysis observed in mild TFP deficiency.[37] One uncommon morbidity of both LCHADD and TFP deficiency is hypoparathyroidism.[38]

Mild TFP deficiency is uncommon and has a peculiar phenotype that shares characteristics with spinal muscular atrophy and inherited sensory-motor neuropathies.[34,36] In addition to symmetric weakness in the wrist and finger extensors, there is a gradual peripheral polyneuropathy that primarily affects the lower limbs starting in infancy or early childhood.[4] Exercise intolerance, planovalgus deformities, bilateral Achilles tendon contractures, and loss of vibratory sensation are potential manifestations.

Acute fatty liver of pregnancy and hemolysis, elevated liver enzymes, and low platelets (HELLP) syndrome can occur in heterozygous pregnant female carriers of TFP mutations carrying a homozygously affected offspring.[11] The pathophysiology of all these extra issues with TFP defects is unknown, but it could be caused by the hazardous accumulation of 3-hydroxy fatty acid intermediates or by unidentified FAO pathway requirements in the retinal, placental, and neurological tissues.[11] Remarkably, none of the other FAO abnormalities have been linked to maternal HELLP syndrome.[17]

While some mutations in the *HADHA* or *HADHB* cause deficiencies in all three enzymes, the prevalent c.1528G>C *HADHA* mutation causes solely LCHADD.[34,37] Patients with mutations in both the *HADHA* and *HADHB* genes exhibit comparably diverse clinical symptoms, making clinical distinction between them impossible. Patients with LCHADD exhibit a variety of phenotypes despite having the same genotype, indicating the significance of other genetic and environmental variables.[35]

Medium-chain Acyl-CoA Dehydrogenase Deficiency

The most prevalent FAO condition is MCADD.[17] MCADD presents as primary hepatic failure accompanied by encephalopathy (Reye-like syndrome) characterized by moderately hypoketotic hypoglycemia.[39] The initial attack is fatal in 20% of cases.[40] According to reports, the death rate within the first 72 hours is 4%.[41] Patients with homozygous c.985A>G mutation have a severe genotype.[3] It should be noted that patients with MCADD may have ketones in their urine when tested with dipsticks during catabolic episodes.[11] This is hypothesised to result from the partial oxidation of long-chain acyl-CoAs to medium-chain acyl-CoAs, producing acetyl-CoA. Although there have been a few anecdotal reports of both cardiac and muscle complications, cardiac, renal, and skeletal muscle signs and symptoms have not yet been demonstrated to contribute to the MCADD phenotype.[40] It is possible that partial oxidation of long-chain fatty acids supplies enough acetyl-CoA to fulfill the requirements of skeletal and cardiac tissues in the great majority of MCADD patients.

Multiple Acyl-CoA Dehydrogenase Deficiency

Deficiencies of either electron transfer flavoprotein (ETF) or ETF-ubiquinone oxidoreductase (ETF-QO), result in MADD, a disorder of fatty acid, amino acid, and choline oxidation.[4] In addition to leg weakness and exercise intolerance with sporadic rhabdomyolysis, patients may exhibit cyclical vomiting, loss of appetite, and proximal muscle weakness affecting the neck, shoulders, hips, and/or respiratory muscles. Acute encephalopathy may be observed in certain patients.[4]

Three clinical phenotypes have been attributed to MADD; a mild or late-onset form, a neonatal form with congenital anomalies, and a neonatal form without congenital malformations.[17] Within the first 24 to 48 hours following a preterm birth, the first group of patients typically exhibits symptoms such as severe non-ketotic hypoglycemia, hypotonia, hepatomegaly, and deep metabolic acidosis. Numerous congenital anomalies, such as multicystic dysplastic kidney, sandal-foot deformity, external genital anomalies, and facial anomalies including low-set ears, large foreheads, hypertelorism, and hypoplastic facial features, are associated with this phenotype. It is believed that the accumulation of metabolites during pregnancy causes dysmorphic characteristics. Within the first twenty-four hours, the second group presents with hypotonia, tachypnea, hepatomegaly, metabolic acidosis, and hypoketotic hypoglycemia. Within the first week, the majority of these individuals die. Patients with severe cardiomyopathy survive only a few months despite prompt diagnosis and meticulous therapy. The third group of patients exhibits various clinical manifestations. In the initial months, these patients may exhibit hypoketotic hypoglycemia, metabolic acidosis, and sporadic vomiting episodes; in adulthood, they may develop Reye-like syndrome and proximal myopathy.[42] High-dose riboflavin treatment has been shown to be beneficial for patients with a moderate clinical presentation.

Riboflavin, also known as vitamin B2, is a precursor of flavin adenine dinucleotide (FAD), a cofactor of numerous dehydrogenases involved in cellular metabolism, including acyl-CoA dehydrogenases in FAO. Notably, riboflavin cannot be synthesized in the human body. Therefore, riboflavin is absorbed by the intestines from the diet, transported through the bloodstream, and taken up by tissue-specific riboflavin transporters. Inside the cell, riboflavin kinase converts riboflavin into flavin mononucleotide (FMN). FMN is adenylated to FAD-by-FAD synthase, encoded by FLAD1. Recently, mutations in FLAD1 were reported to cause a novel form of MADD.

Riboflavin transporter deficiency, comprising *RFVT1* and *RFVT2* (caused by biallelic pathogenic variants in *SLC52A2* and *SLC52A3*, respectively), is a rare neurologic condition characterized by progressive peripheral and cranial neuronopathy causing muscle weakness, with consequent respiratory compromise, vision loss, deafness, and sensory ataxia. The acylcarnitine profile in the blood is abnormal, with accumulation of short- and medium-chain (and sometimes long-chain) acylcarnitines. This can lead to patients being misdiagnosed with MADD. The diagnosis of *RFVT1* and *RFVT2* is established in an individual who has suggestive findings and biallelic pathogenic variants in either *SLC52A2* or *SLC52A3*.

The majority of these riboflavin-responsive MADD patients have been shown to have *ETF-DH* gene mutations, with the majority of these mutations occurring close to the ubiquinone binding pocket.[43] The precursor of FAD is riboflavin, and the capacity of FAD to function as a chemical chaperone that encourages the folding of specific misfolded ETF-QO proteins leads to riboflavin responsiveness.[36] Supplementing with riboflavin aids patients with specific mutations in the *ETF-DH* gene restore residual activity to a greater degree.[43] When riboflavin is administered, the clinical effect is typically rapid and apparent. The majority of patients are young adults or teens.[36]

Short Chain Acyl-CoA Dehydrogenase Deficiency

Short chain acyl-CoA dehydrogenase (SCAD) deficiency is now considered as a biochemical phenotype of uncertain clinical importance, despite the fact that it causes disruptions in certain metabolites consistent with an FAOD.[44] The pathogenesis of SCAD deficiency is poorly understood, and the condition's signs and symptoms have been incredibly variable.[45] Neurological, myopathic, and hepatic signs and symptoms were included in the very first description. Short-chain fatty acid intermediates were thought to cause neurological symptoms because they are volatile and more likely to cross the blood–brain barrier, but this hasn't been proven despite the availability of an animal model.[46] The majority of detected neonates with SCAD deficiency do not develop a clinical phenotype, according to current experience with diagnosis based on newborn screening.[47] Concerns have been raised about patients with SCAD deficiency being mistakenly classified as having a metabolic disorder and that using this as a diagnostic endpoint could lead to inadequate research into the underlying reasons of any symptoms[11].

DIAGNOSIS

Clinicians examining a patient with a preliminary diagnosis of FAOD should be aware of potential pitfalls that can lead to misdiagnosis. Since the FAO pathway is not active when the patient is clinically stable and normoglycaemic, the accumulation of pathological intermediate metabolites will not be significant. To obtain the most useful information about the patient's metabolic status, samples should be collected during metabolic decompensation, for example, at the time of presentation to the emergency department. Samples should be collected as soon as possible after the patient's presentation, before biochemical stabilisation is achieved. With correction of hypoglycemia, abnormal levels of intermediate metabolites will also rapidly return to normal.

The investigation should begin with tests that identify which tissues are affected during the attack and indicate which approach should be taken. These tests include blood gas

analysis, plasma or serum electrolyte measurements, glucose, lactate, and ammonia levels, liver function tests, creatine kinase levels, and urine ketone measurements.

Due to defective FAO, ketone synthesis is impaired. Consequently, even in cases of hypoglycemia resulting from catabolic processes in these patients, urinary ketone levels remain abnormally low (hypoketotic hypoglycemia). In the urine organic acid analysis, an increase in medium-chain dicarboxylic acid levels is observed alongside low ketone levels. Ketone positivity may be present in the urine of patients with MCADD owing to the metabolism of acetyl-CoA, which is produced by the partial oxidation of long-chain fatty acids.

When samples are collected for routine laboratory tests, it is appropriate to also collect samples for metabolic disease diagnostic tests to be performed in the second stage. These include measurements of carnitine (total and free), acylcarnitines, free fatty acids, beta-hydroxybutyrate, and acetoacetate in plasma and serum. Findings that may be observed in plasma acylcarnitine and urine organic acid analyses of FAODs are summarised in Table 1.

It is generally assumed that an abnormal acylcarnitine profile reflects the intramitochondrial accumulation of acyl-CoAs and, as such, indicates the substrate of the deficient enzyme in vivo. The accumulating acyl-CoAs are exported from the mitochondria as acylcarnitines via CPT-II, carnitine acetyltransferase, and CACT. The molecular mechanism of acylcarnitine export across the cell membrane is unresolved.

Rapid confirmation of a particular suspected enzyme deficiency can be performed in lymphocytes, as these cells express all enzymes involved in FAO.

Mutations causing certain diseases have been identified in FAODs. A variety of methodologies have been developed to facilitate mutation analysis using diverse biological samples. Mutation screening can be performed on samples obtained from whole blood or newborn screening cards. The identification of disease-causing mutations through genetic analysis serves to confirm the biochemical diagnosis. Furthermore, in the context of disease forms characterised by a genotype-phenotype relationship, it can provide prognostic insights and inform treatment decisions. This information is of particular significance for genetic counselling and preimplantation genetics.

TREATMENT

The extent to which FAO occurs is primarily determined by the rate of lipolysis in adipose tissue. Preventing prolonged starvation and administering emergency treatment regimens during intercurrent infections reduce FAO. Even in the fed state, cardiac and skeletal muscles use long-chain fatty acids as an energy

Table 1. Laboratory findings in fatty acid oxidation disorders.

	Plasma				Urine	
	Carnitine		Acyl-carnitine	C_{8}-C_{18} FFA	Organic acids	Acyl-glycine
	Co	AC/Co				
Membrane bound enzymes						
Carnitine transporter defect	↓	N	↓	N	N	N
CPT-I deficiency	N/↑	N	N	N	N	N
CACT deficiency	N/↓	↑	+	N	N	N
CPT-II deficiency (neonatal)	N/↓	↑	+	N	N	N
CPT-II deficiency (late onset)	N/↓	↑	+	N	N	N
VLCAD deficiency	N/↓	↑	+	+	+ (acute)	N
ETF-DH (MADD)	N/↓	↑	+	+	+	+
TFP deficiency	N/↓	↑	+ (acute)	+	+ (acute)	N
Mitochondrial matrix enzymes						
MCAD deficiency	N/↓	↑	+	+	+ (acute)	+
SCAD deficiency	N/↓	↑	+	N	+ (acute)	+
ETF-A (MADD)	N/↓	↑	+	+	+	+
ETF-B (MADD)	N/↓	↑	+	+	+	+

AC, acyl-carnitines; CACT, carnitine acylcarnitine translocase; CPT-I, carnitine palmitoyltransferase-I; CPT-II, carnitine palmitoyltransferase-II; ETF-A, electron transfer flavoprotein α subunit; ETF-B, electron transfer flavoprotein β subunit; ETF-DH, electron transfer flavoprotein dehydrogenase; FFA, free fatty acid; MADD, multiple acyl-CoA dehydrogenase; MCAD, medium-chain acyl-CoA dehydrogenase; SCAD, short-chain acyl-CoA dehydrogenase; TFP, trifunctional protein; VLCAD, very long-chain acyl-CoA dehydrogenase.

source. To minimise this, diets containing low amounts of long-chain fatty acids are implemented. When FAOD is suspected, the primary goal is to provide sufficient glucose to prevent lipolysis in target tissues. The main principles of nutritional therapy are as follows: calorie intake in the form of carbohydrates should be provided at regular intervals to prevent both hypoglycemia and the mobilisation of long-chain fatty acids from stores. When the proportion of long-chain fatty acids in the diet is reduced, essential fatty acid supplementation should be provided to prevent deficiency.

For patients with long-chain FAO defects, high-carbohydrate diets are insufficient to ensure adequate caloric intake. To solve this issue, medium-chain triglycerides (MCTs) offer a significant amount of the energy in the diet.[2] Many patients with a defect in one of the long-chain-specific enzymes receive dietary long-chain triglyceride restriction and MCT supplementation, which, in theory, would limit the supply of long-chain fatty acids whose degradation is impaired and provide, as an alternative, a medium-chain fatty acid substrate that can bypass the enzymatic defect. The assumption that 8-, 10-, and 12-carbon fatty acids can enter the mitochondria independently of the carnitine cycle underlies the recommendation to use MCT in the diet. MCTs' well-established ketogenic properties should be beneficial in long-chain FAODs. However, it is unclear whether MCTs should be provided continuously, or only immediately before or during periods of elevated energy demand. In fact, research on *VLCAD* KO mice indicates that while long-term MCT administration caused tissue fat buildup, MCTs are advantageous before exercise.[48] Furthermore, MCT supplementation before exercise enhanced heart function and substrate oxidation in patients with long-chain FAODs.[49]

One theory is that catalytic intermediate leakage from the TCA cycle is the cause of the heart and muscular disease in FAODs.[50] This theory led to the production of triheptanoin, a novel MCT that produces both acetyl-CoA and anaplerotic propionyl-CoA when the heptanoate is oxidized. Ketone bodies like beta-hydroxybutyrate and betahydroxypentoate can be produced from heptanoate.[51] The liver produces ketone bodies, which are then released into the bloodstream and absorbed by various tissues where they can be utilized as TCA cycle substrates and intermediates.[52] Remarkably, a fasting-induced impairment in anaplerosis was validated by recent research in the *LCAD* KO mice, and patients with an FAOD showed clinical improvement after receiving triheptanoin.[50,53]

Although the main treatment for carnitine transporter insufficiency is oral l-carnitine supplementation, it also helps remove harmful metabolites and prevents carnitine shortage in other FAODs. Heart and skeletal muscle tissues contain about 98% of the body's carnitine.[54] Carnitine transporters mediate the uptake of orally administered carnitine into cardiac and skeletal muscle. A single oral dose of l-carnitine has a half-life of 60.3±15 minutes, and regular oral ingestion is necessary to maintain carnitine levels.[54] Although patients with CTD take carnitine supplements, their plasma carnitine levels increase but do not fully normalize. For people with CTD, high-dose carnitine supplementation (up to 200–250 mg/kg/day) is typically necessary. Tissue carnitine levels are not reflected in plasma levels during use of oral l-carnitine supplements. It has been demonstrated that people with CTD have reduced beta oxidation capacity during exercise, which is somewhat recovered by carnitine supplementation.[55] Regrettably, excessive doses of carnitine supplements cause sweat, urine, and breath to smell fishy.

Patients with the *ETF-DH* mutation who have late-onset type MADD typically response favorably to coenzyme Q_{10} and riboflavin.[56]

Carnitine supplementation is frequently used to treat secondary carnitine deficiency in patients with other FAODs. The use of carnitine has been controversial due to the link between acylcarnitines and ventricular fibrillation in a cat model of acute ischemia.[57] Studies on animals reveal both negative and positive effects of carnitine.[58] Studies on humans that are currently available have not demonstrated positive effects.[57]

Footnotes

Conflict of Interest: The author(s) have no conflicts of interest to declare.

Financial Disclosure: The author(s) declared that this study received no financial support.

REFERENCES

1. Kunau WH, Dommes V, Schulz H. Beta-oxidation of fatty acids in mitochondria, peroxisomes, and bacteria: A century of continued progress. Prog Lipid Res. 1995;34(4):267-342. doi: 10.1016/0163-7827(95)00011-9
2. Houten SM, Violante S, Ventura FV, Wanders RJ. The biochemistry and physiology of mitochondrial fatty acid β-oxidation and its genetic disorders. Annu Rev Physiol. 2016;78:23-44. doi: 10.1146/annurev-physiol-021115-105045
3. Janeiro P, Jotta R, Ramos R, Florindo C, Ventura FV, Vilarinho L, de Almeida IT, Gaspar A. Follow-up of fatty acid β-oxidation disorders in expanded newborn screening era. Eur J Pediatr. 2019;178(3):387-394. doi: 10.1007/s00431-018-03315-2
4. Olpin SE. Pathophysiology of fatty acid oxidation disorders and resultant phenotypic variability. J Inherit Metab Dis. 2013;36(4):645-658. doi: 10.1007/s10545-013-9611-5
5. Saudubray JM, Martin D, de Lonlay P, Touati G, Poggi-Travert F, Bonnet D, Jouvet P, Boutron M, Slama A, Vianey-Saban C, Bonnefont JP, Rabier D, Kamoun P, Brivet M. Recognition and management of fatty acid oxidation defects: A series of 107 patients. J Inherit Metab Dis. 1999;22(4):488-502. doi: 10.1023/a:1005556207210

6. Baruteau J, Sachs P, Broué P, Brivet M, Abdoul H, Vianey-Saban C, Ogier de Baulny H. Clinical and biological features at diagnosis in mitochondrial fatty acid beta-oxidation defects: A French pediatric study of 187 patients. J Inherit Metab Dis. 2013;36(5):795-803. doi: 10.1007/s10545-012-9542-6

7. Derks TGJ, Reijngoud DJ, Waterham HR, Gerver WJM, van den Berg MP, Sauer PJJ, Smit GPA. The natural history of medium-chain acyl CoA dehydrogenase deficiency in the Netherlands: Clinical presentation and outcome. J Pediatr. 2006;148(5):665-670. doi: 10.1016/j.jpeds.2005.12.028

8. Laforêt P, Acquaviva-Bourdain C, Rigal O, Brivet M, Penisson-Besnier I, Chabrol B, Chaigne D, Boespflug-Tanguy O, Laroche C, Bedat-Millet AL, Behin A, Eymard B, Vianey-Saban C. Diagnostic assessment and long-term follow-up of 13 patients with very long-chain acyl-coenzyme A dehydrogenase (VLCAD) deficiency. Neuromuscul Disord. 2009;19(5):324-329. doi: 10.1016/j.nmd.2009.02.007

9. den Boer ME, Dionisi-Vici C, Chakrapani A, van Thuijl AOJ, Wanders RJA, Wijburg FA. Mitochondrial trifunctional protein deficiency: A severe fatty acid oxidation disorder with cardiac and neurologic involvement. J Pediatr. 2003;142(6):684-689. doi: 10.1067/mpd.2003.231

10. Fletcher AL, Pennesi ME, Harding CO, Weleber RG, Gillingham MB. Observations regarding retinopathy in mitochondrial trifunctional protein deficiencies. Mol Genet Metab. 2012;106(1):18-24. doi: 10.1016/j.ymgme.2012.02.015

11. Bennett MJ. Pathophysiology of fatty acid oxidation disorders. J Inherit Metab Dis. 2010;33(5):533-537. doi: 10.1007/s10545-010-9170-y

12. Lopaschuk GD, Ussher JR, Folmes CDL, Jaswal JS, Stanley WC. Myocardial fatty acid metabolism in health and disease. Physiol Rev. 2010;90(1):207-258. doi: 10.1152/physrev.00015.2009

13. Barger PM, Kelly DP. PPAR signaling in the control of cardiac energy metabolism. Trends Cardiovasc Med. 2000;10(6):238-245. doi: 10.1016/s1050-1738(00)00077-3

14. Helge JW, Stallknecht B, Richter EA, Galbo H, Kiens B. Muscle metabolism during graded quadriceps exercise in man. J Physiol. 2007;581(Pt 3):1247-1258. doi: 10.1113/jphysiol.2007.128348

15. Strauss AW, Bennett MJ. Mitochondrial fatty acid oxidation defects. In: Sarafoglou K, Hoffmann GF, Roth KS, editors. Pediatric Endocrinology and Inborn Errors of Metabolism. McGraw-Hill; 2009:51-70.

16. Thuillier L, Rostane H, Droin V, Demaugre F, Brivet M, Kadhom N, Prip-Buus C, Gobin S, Saudubray JM, Bonnefont JP. Correlation between genotype, metabolic data, and clinical presentation in carnitine palmitoyltransferase 2 (CPT2) deficiency. Hum Mutat. 2003;21(5):493-501. doi: 10.1002/humu.10201

17. Spiekerkoetter U. Mitochondrial fatty acid oxidation disorders: Clinical presentation of long-chain fatty acid oxidation defects before and after newborn screening. J Inherit Metab Dis. 2010;33(5):527-532. doi: 10.1007/s10545-010-9090-x

18. Spiekerkoetter U, Huener G, Baykal T, Demirkol M, Duran M, Wanders R, Nezu J, Mayatepek E. Silent and symptomatic primary carnitine deficiency within the same family due to identical mutations in the organic cation/carnitine transporter OCTN2. J Inherit Metab Dis. 2003;26(6):613-615. doi: 10.1023/a:1025968502527

19. Tein I. Carnitine transport: Pathophysiology and metabolism of known molecular defects. J Inherit Metab Dis. 2003;26(2-3):147-169. doi: 10.1023/a:1024481016187

20. Rose EC, di San Filippo CA, Ndukwe Erlingsson UC, Ardon O, Pasquali M, Longo N. Genotype-phenotype correlation in primary carnitine deficiency. Hum Mutat. 2012;33(1):118-123. doi: 10.1002/humu.21607

21. Price N, van der Leij F, Jackson V, Corstorphine C, Thomson R, Sorensen A, Zammit V. A novel brain-expressed protein related to carnitine palmitoyltransferase I. Genomics. 2002;80(4):433-442. doi: 10.1006/geno.2002.6845

22. Weis BC, Esser V, Foster DW, McGarry JD. Rat heart expresses two forms of mitochondrial carnitine palmitoyltransferase I. The minor component is identical to the liver enzyme. J Biol Chem. 1994;269(29):18712-18715.

23. Falik-Borenstein ZC, Jordan SC, Saudubray JM, Brivet M, Demaugre F, Edmond J, Cederbaum SD. Brief report: Renal tubular acidosis in carnitine palmitoyltransferase type 1 deficiency. N Engl J Med. 1992;327(1):24-27. doi: 10.1056/nejm199207023270105

24. Hug G, Bove KE, Soukup S. Lethal neonatal multiorgan deficiency of carnitine palmitoyltransferase II. N Engl J Med. 1991;325(26):1862-1864. doi: 10.1056/nejm199112263252607

25. Demaugre F, Bonnefont JP, Mitchell G, Nguyen-Hoang N, Pelet A, Rimoldi M, Di Donato S, Saudubray JM. Hepatic and muscular presentations of carnitine palmitoyl transferase deficiency: Two distinct entities. Pediatr Res. 1988;24(3):308-311. doi: 10.1203/00006450-198809000-00006

26. Corado JAM, Lee CU, Enns GM. Carnitine-acylcarnitine translocase deficiency. 2025. https://www.ncbi.nlm.nih.gov/books/NBK582032/

27. Longo N, Amat di San Filippo C, Pasquali M. Disorders of carnitine transport and the carnitine cycle. Am J Med Genet C Semin Med Genet. 2006;142C(2):77-85. doi: 10.1002/ajmg.c.30087

28. Andresen BS, Bross P, Vianey-Saban C, Divry P, Zabot MT, Roe CR, Nada MA, Byskov A, Kruse TA, Neve S, Kristiansen K, Knudsen I, Corydon MJ, Gregersen N. Cloning and characterization of human very-long-chain acyl-CoA dehydrogenase cDNA, chromosomal assignment of the gene and identification in four patients of nine different mutations within the VLCAD gene. Hum Mol Genet. 1996;5(4):461-472. doi: 10.1093/hmg/5.4.461

29. Marsden D, Bedrosian CL, Vockley J. Impact of newborn screening on the reported incidence and clinical outcomes associated with medium- and long-chain fatty acid oxidation disorders. Genet Med. 2021;23(5):816-829. doi: 10.1038/s41436-020-01070-0

30. Schiff M, Mohsen AW, Karunanidhi A, McCracken E, Yeasted R, Vockley J. Molecular and cellular pathology of very-long-chain acyl-CoA dehydrogenase deficiency. Mol Genet Metab. 2013;109(1):21-27. doi: 10.1016/j.ymgme.2013.02.002

31. Boneh A, Andresen BS, Gregersen N, Ibrahim M, Tzanakos N, Peters H, Yaplito-Lee J, Pitt JJ. VLCAD deficiency: Pitfalls in newborn screening and confirmation of diagnosis by mutation analysis. Mol Genet Metab. 2006;88(2):166-170. doi: 10.1016/j.ymgme.2005.12.012

32. Hoffmann L, Haussmann U, Mueller M, Spiekerkoetter U. VLCAD enzyme activity determinations in newborns identified by screening: A valuable tool for risk assessment. J Inherit Metab Dis. 2012;35(2):269-277. doi: 10.1007/s10545-011-9391-8

33. Liebig M, Schymik I, Mueller M, Wendel U, Mayatepek E, Ruiter J, Strauss AW, Wanders RJA, Spiekerkoetter U. Neonatal screening for very long-chain acyl-CoA dehydrogenase deficiency: Enzymatic and molecular evaluation of neonates with elevated C14:1-carnitine levels. Pediatrics. 2006;118(3):1065-1069. doi: 10.1542/peds.2006-0666

34. Spiekerkoetter U, Bennett MJ, Ben-Zeev B, Strauss AW, Tein I. Peripheral neuropathy, episodic myoglobinuria, and respiratory failure in deficiency of the mitochondrial trifunctional protein. Muscle Nerve. 2004;29(1):66-72. doi: 10.1002/mus.10500

35. den Boer ME, Wanders RJ, Morris AA, Ijlst L, Heymans HS, Wijburg FA. Long-chain 3-hydroxyacyl-CoA dehydrogenase deficiency: Clinical presentation and follow-up of 50 patients. Pediatrics. 2002;109(1):99-104. doi: 10.1542/peds.109.1.99

36. Olpin SE, Clark S, Andresen BS, Bischoff C, Olsen RKJ, Gregersen N, Chakrapani A, Downing M, Manning NJ, Sharrard M, Bonham JR, Muntoni F, Turnbull DM, Pourfarzam M. Biochemical, clinical and molecular findings in LCHAD and general mitochondrial trifunctional protein deficiency. J Inherit Metab Dis. 2005;28(4):533-544. doi: 10.1007/s10545-005-0533-8

37. Spiekerkoetter U, Sun B, Zytkovicz T, Wanders R, Strauss AW, Wendel U. MS/MS-based newborn and family screening detects asymptomatic patients with very-long-chain acyl-CoA dehydrogenase deficiency. J Pediatr. 2003;143(3):335-342. doi: 10.1067/s0022-3476(03)00292-0

38. Tyni T, Kivelä T, Lappi M, Summanen P, Nikoskelainen E, Pihko H. Ophthalmologic findings in long-chain 3-hydroxyacyl-CoA dehydrogenase deficiency caused by the G1528C mutation: A new type of hereditary metabolic chorioretinopathy. Ophthalmology. 1998;105(5):810-824. doi: 10.1016/s0161-6420(98)95019-9

39. Rinaldo P, Matern D, Bennett MJ. Fatty acid oxidation disorders. Annu Rev Physiol. 2002;64:477-502. doi: 10.1146/annurev.physiol.64.082201.154705

40. Iafolla AK, Thompson RJ Jr, Roe CR. Medium-chain acyl-coenzyme A dehydrogenase deficiency: Clinical course in 120 affected children. J Pediatr. 1994;124(3):409-415. doi: 10.1016/s0022-3476(94)70363-9

41. Wilcken B. Fatty acid oxidation disorders: Outcome and long-term prognosis. J Inherit Metab Dis. 2010;33(5):501-506. doi: 10.1007/s10545-009-9001-1

42. Dusheiko G, Kew MC, Joffe BI, Lewin JR, Mantagos S, Tanaka K. Recurrent hypoglycemia associated with glutaric aciduria type II in an adult. N Engl J Med. 1979;301(26):1405-1409. doi: 10.1056/nejm197912273012601

43. Olsen RK, Olpin SE, Andresen BS, Miedzybrodzka ZH, Pourfarzam M, Merinero B, Frerman FE, Beresford MW, Dean JC, Cornelius N, Andersen O, Oldfors A, Holme E, Gregersen N, Turnbull DM, Morris AA. ETFDH mutations as a major cause of riboflavin-responsive multiple acyl-CoA dehydrogenation deficiency. Brain. 2007;130(Pt 8):2045-2054. doi: 10.1093/brain/awm135

44. Coates PM, Hale DE, Finocchiaro G, Tanaka K, Winter SC. Genetic deficiency of short-chain acyl-coenzyme A dehydrogenase in cultured fibroblasts from a patient with muscle carnitine deficiency and severe skeletal muscle weakness. J Clin Invest. 1988;81(1):171-175. doi: 10.1172/jci113290

45. Jethva R, Bennett MJ, Vockley J. Short-chain acyl-coenzyme A dehydrogenase deficiency. Mol Genet Metab. 2008;95(4):195-200. doi: 10.1016/j.ymgme.2008.09.007

46. Wood PA, Amendt BA, Rhead WJ, Millington DS, Inoue F, Armstrong D. Short-chain acyl-coenzyme A dehydrogenase deficiency in mice. Pediatr Res. 1989;25(1):38-43. doi: 10.1203/00006450-198901000-00010

47. Jethva R, Ficicioglu C. Clinical outcomes of infants with short-chain acyl-coenzyme A dehydrogenase deficiency (SCADD) detected by newborn screening. Mol Genet Metab. 2008;95(4):241-242. doi: 10.1016/j.ymgme.2008.09.003

48. Primassin S, Tucci S, Herebian D, Seibt A, Hoffmann L, ter Veld F, Spiekerkoetter U. Pre-exercise medium-chain triglyceride application prevents acylcarnitine accumulation in skeletal muscle from very-long-chain acyl-CoA-dehydrogenase-deficient mice. J Inherit Metab Dis. 2010;33(3):237-246. doi: 10.1007/s10545-010-9105-7

49. Behrend AM, Harding CO, Shoemaker JD, Matern D, Sahn DJ, Elliot DL, Gillingham MB. Substrate oxidation and cardiac performance during exercise in disorders of long-chain fatty acid oxidation. Mol Genet Metab. 2012;105(1):110-115. doi: 10.1016/j.ymgme.2011.09.030

50. Roe CR, Sweetman L, Roe DS, David F, Brunengraber H. Treatment of cardiomyopathy and rhabdomyolysis in long-chain fat oxidation disorders using an anaplerotic odd-chain triglyceride. J Clin Invest. 2002;110(2):259-269. doi: 10.1172/jci15311

51. Gu L, Zhang GF, Kombu RS, Allen F, Kutz G, Brewer WU, Roe CR, Brunengraber H. Parenteral and enteral metabolism of anaplerotic triheptanoin in normal rats. II. Effects on lipolysis, glucose production, and liver acyl-CoA profile. Am J Physiol Endocrinol Metab. 2010;298(2):E362-E371. doi: 10.1152/ajpendo.00384.2009

52. Lee SK, Gupta M, Shi J, McKeever K. The pharmacokinetics of triheptanoin and its metabolites in healthy subjects and patients with long-chain fatty acid oxidation disorders. Clin Pharmacol Drug Dev. 2021;10(11):1325-1334. doi: 10.1002/cpdd.944

53. Roe CR, Yang BZ, Brunengraber H, Roe DS, Wallace M, Garritson BK. Carnitine palmitoyltransferase II deficiency: Successful anaplerotic diet therapy. Neurology. 2008;71(4):260-264. doi: 10.1212/01.wnl.0000318283.42961.e9

54. Ambrose A, Sheehan M, Bahl S, Athey T, Ghai-Jain S, Chan A, Shoemaker J. Outcomes of mitochondrial long-chain fatty acid oxidation and carnitine defects from a single center metabolic genetics clinic. Orphanet J Rare Dis. 2022;17(1):360. doi: 10.1186/s13023-022-02512-5

55. Madsen KL, Preisler N, Rasmussen J, Hedermann G, Olesen JH, Lund AM, Vissing J. L-Carnitine improves skeletal muscle fat oxidation in primary carnitine deficiency. J Clin Endocrinol Metab. 2018;103(12):4580-4588. doi: 10.1210/jc.2018-00953

56. Missaglia S. New perspectives in late-onset multiple acyl-CoA dehydrogenase deficiency: Clinical and genetic findings. J Neurol Sci. 2023;455:122809. doi: 10.1016/j.jns.2023.122809

57. Spiekerkoetter U, Bastin J, Gillingham M, Morris A, Wijburg F, Wilcken B. Current issues regarding treatment of mitochondrial fatty acid oxidation disorders. J Inherit Metab Dis. 2010;33(5):555-561. doi: 10.1007/s10545-010-9188-1

58. Primassin S, ter Veld F, Mayatepek E, Spiekerkoetter U. Carnitine supplementation induces acylcarnitine production in tissues of very long-chain acyl-CoA dehydrogenase-deficient mice, without replenishing low free carnitine. Pediatr Res. 2008;63(6):632-637. doi: 10.1203/PDR.0b013e31816ff6f0

REVIEW

DOI: 10.4274/imdn.galenos.2026.2026-6

Inherit Metab Disord Nutr 2026;2:25–30

Mucopolysaccharidosis Type II (Hunter Syndrome): A Brief Review of Pathophysiology, Clinical Spectrum, and Current Therapeutic Strategies

Havva Yazıcı

Ege University Faculty of Medicine, Department of Pediatrics, Division of Pediatric Metabolism, İzmir, Türkiye

Abstract

Mucopolysaccharidosis type II (MPS II, Hunter syndrome) is a rare, X-linked lysosomal storage disorder caused by a deficiency of iduronate-2-sulfatase, resulting in progressive accumulation of heparan sulfate and dermatan sulfate in multiple tissues. The disease presents as a broad clinical spectrum ranging from attenuated forms with preserved cognitive function to severe neuronopathic forms characterized by progressive neurodegeneration. Common clinical manifestations include coarse facial features, hepatosplenomegaly, skeletal abnormalities, cardiac valve disease, airway obstruction, hearing loss, and neurological impairment. The diagnosis is established by demonstrating deficient enzyme activity and by molecular confirmation of pathogenic variants in the *IDS* gene. Intravenous enzyme replacement therapy has significantly improved somatic manifestations and the quality of life; however, its inability to cross the blood–brain barrier limits its effectiveness in preventing neurological disease progression. Recent advances, including hematopoietic stem cell transplantation, blood–brain barrier-penetrating enzyme replacement therapies, intrathecal and intracerebroventricular enzyme administration, and gene therapy, offer promising approaches to address central nervous system involvement. This review summarizes the current understanding of the pathophysiology, clinical spectrum, diagnosis, and evolving therapeutic strategies for MPS II, with particular emphasis on emerging treatments targeting neurological disease.

Keywords: Mucopolysaccharidosis type II; Hunter syndrome; Lysosomal storage disorder; Enzyme replacement therapy; Gene therapy; Newborn screening

INTRODUCTION

Mucopolysaccharidosis type II (MPS II, Hunter syndrome) is a rare, X-linked recessive, multisystemic, and progressive lysosomal storage disorder.[1] The disease was first described in 1917 by Canadian physician Charles A. Hunter in two male siblings. Hunter characterized them as having severe somatic manifestations, including macrocephaly, dysmorphic facial features, hepatosplenomegaly, joint contractures, hearing impairment, noisy breathing, and cardiomegaly, despite having normal intelligence. The term mucopolysaccharidosis was introduced by Brante in 1952, and the biochemical basis of the disease was established in 1968 when Fratantoni et al. described the *in vitro* phenomenon of cross-correction, demonstrating that enzyme-deficient cells could be functionally corrected by enzyme-producing cells.[2] The core biochemical defect is a deficiency of the enzyme iduronate-2- sulfatase (I2S) (EC 3.1.6.13), which plays a vital role in the lysosomal catabolism of glycosaminoglycans (GAGs). Specifically, I2S catalyzes the hydrolysis of the C-2 sulfate ester bond at the non-reducing terminal L-iduronic acid residues of dermatan sulfate (DS) and heparan sulfate (HS). The reduction or complete absence of I2S activity leads to the massive, progressive accumulation of partially degraded HS and DS within the lysosomes of virtually every cell type in the body, as well as within the extracellular matrix.[2]

Although the progressive lysosomal accumulation of HS and DS is the primary biochemical hallmark of MPS II, the

Address for Correspondence: Havva Yazıcı, MD, Ege University Faculty of Medicine, Department of Pediatrics, Division of Pediatric Metabolism, İzmir, Türkiye

E-mail: havvaya@gmail.com **ORCID ID:** orcid.org/0000-0002-2564-7420

Received: 04.07.2026 **Accepted:** 09.09.2026 **Publication Date:** 30.09.2026

Cite this article as: Yazıcı H. Mucopolysaccharidosis type II (Hunter syndrome): a brief review of pathophysiology, clinical spectrum, and current therapeutic strategies. Inherit Metab Disord Nutr. 2026;2:25–30

Copyright© 2026 The Author(s). Published by Galenos Publishing House on behalf of Child Nutrition Metabolism Association.
This is an open access article under the Creative Commons AttributionNonCommercial 4.0 International (CC BY-NC 4.0) License.

pathological consequences of this storage process extend considerably beyond simple substrate deposition.[3] Increasing evidence suggests that GAG accumulation initiates a complex network of secondary cellular disturbances, including lysosomal dysfunction, impaired autophagy, oxidative stress, and chronic inflammation, which collectively drive tissue injury and multisystem disease progression. The pathophysiology extends far beyond the mere mechanical engorgement of cells by HS and DS, encompassing a destructive cascade of cellular dysfunction and inflammatory signaling. Primary GAG accumulation impairs lysosomal function, thereby inhibiting other acid hydrolases and leading to secondary lysosomal accumulation of neurotoxic and pro-inflammatory molecules, including GM2 and GM3 gangliosides, globotriaosylsphingosine, unesterified cholesterol, and tau proteins.[4] Furthermore, undegraded HS fragments structurally mimic the lipopolysaccharides of Gram-negative bacteria and act as potent ligands for toll-like receptor 4 (TLR4) on the surface of microglia and peripheral macrophages. Activation of the TLR4-MyD88 pathway induces NF-κB signaling and activates the NLRP3 inflammasome, leading to excessive release of pro-inflammatory mediators, including cytokines such as interleukin-1β and tumor necrosis factor-alpha, and matrix metalloproteinases, thereby promoting chronic systemic inflammation and neurodegeneration. In parallel, the massive intracellular GAG burden compromises lysosomal membrane integrity, allowing destructive hydrolases, such as cathepsin B, to leak into the cytosol and accelerate cell death. Simultaneously, disruption of autophagic and mitophagic flux markedly increases intracellular oxidative stress, further exacerbating cellular dysfunction and tissue damage.[5]

This enzyme is encoded by the *IDS* gene, linking the biochemical defect directly to the disease's underlying genetic cause. MPS II is caused by pathogenic variants in the *IDS* gene located at *Xq28* on the X chromosome. The *IDS* gene spans approximately 24 kb, contains nine exons, and encodes a 550-amino acid polypeptide.[6] To date, over 800 distinct pathogenic variants have been identified, including nonsense and missense mutations, splice-site mutations, and major structural alterations. A significant challenge in understanding the genetic architecture is the presence of the IDSP1 pseudogene, located approximately 20-25 kb telomeric to the active *IDS* gene. Sharing up to 100% sequence homology with specific exons of the *IDS* gene, this pseudogene predisposes the locus to unequal homologous recombination events. These events frequently result in complex genetic rearrangements, such as inversions and large deletions, which are characteristically associated with severe disease phenotypes. Although MPS II almost exclusively affects males due to its X-linked recessive inheritance, rare symptomatic female cases have been documented, primarily resulting from skewed X-chromosome inactivation or structural chromosomal abnormalities.[3,7]

Reflecting these underlying genetic drivers, the epidemiological landscape of MPS II demonstrates significant global variation.[7,8] Worldwide, it is recognized as an ultra-rare lysosomal storage disorder, with a reported birth prevalence ranging from 0.13 to 2.16 per 100,000 live births.[9] Striking geographic heterogeneity and ethnicity-driven variations are documented worldwide.[8,10] In East Asian populations—such as Taiwan (1.07/100,000), Japan (0.84/100,000), and South Korea (0.74/100,000)—MPS II represents the predominant subtype, accounting for 50% to 55% of all diagnosed MPS cases.[11-13] This high relative frequency is primarily driven by founder variants, particularly by high allele frequencies of p.R468 alterations and by recurrent IDS–IDSP1 genomic recombinations.[14,15] Conversely, MPS II represents only 4% to 27% of all MPS diagnoses in European and North American populations, with birth prevalence reported as 0.13 per 100,000 in Norway, 0.64 per 100,000 in Germany, and 0.26 per 100,000 in the United States.[12,16] Real-world data from high-throughput newborn screening (NBS) panels indicate that traditional clinical ascertainment has underestimated disease incidence; for example, US screening initiatives revealed a prevalence of 1 in 73,290, higher than historical registry estimates.[17] Owing to its X-linked recessive inheritance pattern, MPS II almost exclusively affects hemizygous males and has a male-specific birth prevalence ranging from 2.05 per 100,000 male live births in Taiwan to 4.2 per 100,000 male live births in Estonia.[11,18] Symptomatic cases in females remain extraordinarily rare, with approximately 24 confirmed cases documented in the global literature. Disease expression in females requires a total loss of functional enzyme activity, which predominantly arises from extremely skewed X-chromosome inactivation (silencing the normal allele), structural X-chromosome rearrangements (e.g., monosomy X/Turner syndrome or X-autosome translocations), or exceptionally rare homozygous inheritance resulting from parental consanguinity.[9]

CLINICAL FINDINGS

MPS II presents as a continuous phenotypic spectrum, driven by the progressive accumulation of GAGs at the cellular and tissue levels. Clinically, the disease is categorized into two main phenotypes based on the presence of neurological involvement and the rate of progression: the severe (neuronopathic) and the attenuated (non-neuronopathic) phenotypes. The neuronopathic form, representing approximately two-thirds of the patient population, typically manifests between 18 and 36 months of age. The severe phenotype is dominated by progressive cognitive and neurobehavioral decline. Conversely, patients with the attenuated form do not experience significant cognitive regression and often survive into adulthood.[19] However, data from the Hunter Outcome Survey (HOS), the largest global registry for patients with MPS II, strongly indicate that patients with the attenuated form experience a somatic disease burden as severe

as that of their neuronopathic counterparts and require frequent surgical interventions for manifestations such as hernias and carpal tunnel syndrome during the first two decades of life.[20] The clinical features of the severe and attenuated phenotypes of MPS II are summarized in Table 1.

The clinical distinction among phenotypic forms is most evident in the extent of neurological involvement, the principal determinant of disease severity and long-term prognosis. Primary neurological involvement is the hallmark of the severe phenotype, presenting as developmental arrest followed by regression, typically beginning at 18–36 months.[7] Elevated levels of neurofilament light chain in cerebrospinal fluid (CSF) and serum have recently been established as robust biomarkers of progressive axonal damage and neurodegeneration. Clinically, this manifests as extreme hyperactivity, aggression, sleep disturbances, and ultimately intractable seizures. Secondary neurological complications arise from GAG deposition in the meninges and neural vasculature, leading to communicating hydrocephalus, cervical spinal stenosis (cervical myelopathy), and carpal tunnel syndrome.[21]

Skeletal dysplasia is largely driven by the accumulation of DS. DS interferes with small leucine-rich proteoglycans, disrupting collagen fibril assembly in the extracellular matrix. Furthermore, accumulated HS competitively inhibits the signaling pathways of fibroblast growth factor and bone morphogenetic protein, both of which are critical for bone morphogenesis. Patients develop restricted joint mobility, claw-hand deformities, short stature, kyphoscoliosis, thickened ribs, and the characteristic skeletal presentation, dysostosis multiplex.[3]

DS is a major component of normal cardiac valves. In MPS II, massive DS deposition within valve leaflets and the myocardium triggers fibrosis and inflammation, leading to severe valvular disease, particularly mitral and aortic regurgitation or stenosis. Left ventricular hypertrophy, arrhythmias, and eventual heart failure follow and together constitute one of the leading causes of mortality.[3,22]

GAG deposition in mucosal tissue causes macroglossia, adenotonsillar hypertrophy, and vocal cord thickening. More critically, tracheobronchomalacia, combined with highly viscous secretions, drastically narrows the upper and lower airways. This leads to progressive obstructive sleep apnea, noisy breathing, difficult intubation, and life-threatening recurrent respiratory infections. Mixed conductive and sensorineural hearing loss is nearly universal, resulting from chronic otitis media, ossicular dysostosis, and cochlear nerve compression.[7]

GAG storage in the reticuloendothelial system results in almost universal hepatosplenomegaly and associated inguinal or umbilical hernias. Pebble-like, ivory-colored skin lesions on the back and upper arms have been reported in MPS II. Notably, unlike MPS I or VI, significant corneal clouding is extremely rare in MPS II.[23] This is hypothesized to result from the protective effect of an extra sulfate group on the DS molecules that accumulate in MPS II.[24]

DIAGNOSIS

Establishing a prompt and precise diagnosis of MPS II requires an integrated approach that combines clinical awareness with targeted biochemical screening, enzymatic confirmation, and molecular characterization.[23] Initial diagnostic evaluation is commonly prompted by overt physical features or an abnormal NBS result. Quantitative assessment of total urinary GAGs (uGAGs) via dye-binding assays offers a useful initial indicator; however, it lacks specificity and may yield false-negative results. To avoid false negatives, qualitative GAG profiling by liquid chromatography–tandem mass spectrometry or urine GAG electrophoresis is preferred for specifically detecting elevated levels of DS and HS.[15,25]

In male patients, definitive biochemical diagnosis relies on demonstrating deficient or completely absent I2S activity in

Table 1. Clinical features of the severe and attenuated phenotypes in mucopolysaccharidosis type II.

Clinical feature/system	Neuronopathic (severe) phenotype	Attenuated phenotype
Prevalence and onset	2/3 of cases; typical onset at 18–36 months	1/3 of cases; typically later onset
Primary CNS disease	Progressive cognitive decline, developmental arrest, hyperactivity, aggression, and intractable seizures	Absent or minimal; preserved cognitive functions and normal neurodevelopmental trajectory
Secondary CNS disease	Communicating hydrocephalus, cervical spinal stenosis, and carpal tunnel syndrome	High risk for hydrocephalus, spinal stenosis, and carpal tunnel syndrome (similar to severe form)
Somatic burden	Severe: Dysostosis multiplex, restricted joint mobility, valvular heart disease, macroglossia, and upper airway obstruction	Marked somatic burden; early surgical interventions are frequently required for hernias and carpal tunnel syndrome
Prognosis	Shortened survival; premature death is typically driven by neurodegeneration and cardiorespiratory failure	Prolonged survival into adulthood; prognosis depends on somatic and valvular complications

CNS, central nervous system.

leukocytes, plasma, or cultured fibroblasts. Dried blood spot enzyme assays have revolutionized early detection by providing a rapid, minimal-volume substrate suitable for both high-throughput NBS and primary diagnostic triage. Notably, it is clinically mandatory to measure the normal activity of at least one other sulfatase to rule out multiple sulfatase deficiency.[15]

Identifying pathogenic variants in the *IDS* gene provides essential genetic confirmation, enables genotype–phenotype predictions, and guides family counseling. Standard Sanger sequencing or targeted next-generation sequencing (NGS) panels effectively detect single- nucleotide variants and small insertions or deletions. Nonetheless, molecular confirmation is often complicated by IDSP1, a *pseudogene* located ~20–25 kb telomeric to IDS and sharing *extensive* sequence identity with IDS. Non-allelic homologous recombination between these loci accounts for 10-15% of pathogenic alleles, producing complex inversions and structural deletions that can easily escape detection by conventional Polymerase Chain Reaction (PCR) or short-read NGS. Resolving these complex genomic rearrangements often requires dedicated techniques such as long-read sequencing, MLPA, or PCR-RFLP analysis.[14,23,26]

Detection of female carriers is a critical component of genetic counseling, as MPS II is inherited in an X-linked recessive pattern in which approximately 92% of mothers of affected males are carriers and ~8% carry de novo mutations.[27] Measurement of I2S enzyme activity or uGAGs in females is clinically unreliable for carrier identification because random X-chromosome inactivation causes significant overlap with normal control ranges. Although most carriers are clinically asymptomatic, skewed X-chromosome inactivation can occasionally result in mild, progressive somatic manifestations—such as joint stiffness, carpal tunnel syndrome, hypoacusia, and skeletal anomalies—warranting longitudinal clinical monitoring.[28] Consequently, targeted molecular genetic testing for the familial IDS variant is the only reliable approach to identify female carriers.[15] Once the proband's mutation is established, direct DNA-based methodologies—including Sanger sequencing, restriction fragment digestion, specialized PCR assays for gene–pseudogene recombinations, and high-sensitivity NGS, capable of detecting low-level somatic or germline mosaicism—enable precise cascade testing of at-risk female relatives and provide essential options for prenatal and preimplantation genetic diagnosis.[14,23,25]

CURRENT TREATMENTS

The therapeutic management of MPS II has historically shifted from palliative, symptom-focused care to disease-specific therapy.[20] Although current treatments significantly alter the somatic course of the disease, addressing the profound neurological burden remains a critical challenge.

Intravenous (IV) administration of recombinant human I2S is the current first-line treatment for MPS II. When administered weekly at a dose of 0.5 mg/kg, IV enzyme replacement therapy (ERT) effectively targets somatic macrophages via mannose-6-phosphate receptor-mediated endocytosis. Clinical trials and extensive real-world registry data, including findings from the HOS, consistently show that ERT rapidly reduces uGAG excretion and normalizes liver and spleen volumes. It also provides measurable improvements or stabilization in functional endurance [e.g., the 6-minute walk test (6MWT)] and pulmonary capacity.[20] While IV ERT effectively manages systemic disease, its inability to penetrate avascular tissues (such as cardiac valves and cartilage) and the central nervous system limits its overall therapeutic efficacy.[29] In addition, avascular or poorly vascularized tissues, such as cardiac valves, bone growth plates, and cartilage, exhibit poor enzyme penetration. Consequently, valvulopathy, airway obstruction, and skeletal dysplasia often continue to progress despite long-term enzymatic treatment.[30] Another important therapeutic limitation is the development of anti-drug antibodies (ADAs), which occur in approximately 50% of treated patients. Although neutralizing ADAs can attenuate biochemical responses, including slower reductions in uGAG levels, their direct impact on functional clinical outcomes, such as the 6MWT, remains variable. Nevertheless, they continue to pose a concern due to infusion-related hypersensitivity reactions.[20]

The role of allogeneic hematopoietic stem cell transplantation (HSCT) in MPS II has historically been controversial. Unlike in MPS I (Hurler syndrome), early HSCT attempts in MPS II were associated with high morbidity and limited preservation of neurocognitive function.[31] However, modern advancements in preconditioning regimens—including targeted busulfan and fludarabine—and improvements in donor matching have significantly reduced procedural mortality.[32] Current evidence suggests that if HSCT is performed very early in the disease course, before the onset of symptoms or before 2 years of age, donor-derived engrafted microglia may provide a continuous source of I2S to the brain parenchyma, potentially stabilizing cognitive decline. Thus, very early HSCT is increasingly recognized as a viable option for carefully selected patients with neuronopathic disease.[33]

CURRENT CHALLENGES, EMERGING FRONTIERS, AND FUTURE DIRECTIONS

Driven by the urgent need to address neuronopathic manifestations, recent therapeutic advances focus on pre-symptomatic detection and drug delivery strategies capable of bypassing the blood–brain barrier (BBB). A major historical hurdle in MPS II has been the diagnostic odyssey during which irreversible CNS and somatic damage occur before treatment is initiated. The inclusion of MPS II in NBS panels, such as the Recommended Uniform Screening Panel in the United States,

represents a monumental shift.[8] However, NBS introduces a complex prognostic challenge: accurately predicting the clinical phenotype from the identified genotype in a pre-symptomatic neonate. While large structural deletions or complex rearrangements reliably predict the severe phenotype, private missense variants or variants of unknown significance complicate clinical decision-making. Accurate phenotypic prediction is imperative, as it dictates the risk-benefit justification for aggressive CNS–targeted early interventions, such as HSCT or experimental gene therapies.[25]

Direct enzyme administration into the CSF through intrathecal or intracerebroventricular (ICV) delivery has emerged as a promising strategy for circumventing BBB limitations. Clinical studies evaluating ICV idursulfase beta, delivered via surgically implanted reservoirs, have demonstrated substantial reductions in CSF HS concentrations, accompanied by stabilization of neurodevelopmental decline, ultimately leading to regulatory approval in selected regions, including Japan.[34] A complementary non-invasive strategy relies on receptor-mediated transcytosis, often described as a "molecular Trojan horse" approach. In this method, the therapeutic I2S enzyme is fused to monoclonal antibodies that target BBB transcytosis receptors, particularly the human transferrin receptor. Following IV administration, receptor binding initiates transcytosis across the cerebrovascular endothelium, facilitating enzyme delivery into the brain parenchyma.[35] Pabinafusp alfa, currently approved in Japan, represents the first systemic ERT to demonstrate dual efficacy by reducing both somatic disease burden and CSF HS levels while stabilizing neurocognitive function. Similar investigational compounds, including tividenofusp alfa, continue to advance through late-stage global clinical development.[8]

Beyond enzyme replacement strategies, next-generation therapeutic modalities increasingly focus on achieving sustained endogenous production of I2S through gene-based approaches. *In vivo* gene therapy using adeno-associated viral (AAV) vectors, particularly AAV9-based platforms such as RGX-121, has demonstrated encouraging early clinical results following intracisternal CNS delivery, including marked reductions in CSF biomarkers and sustained neurodevelopmental acquisition.[34] Alternatively, *ex vivo* lentiviral *hematopoietic stem cell* gene therapy involves harvesting autologous CD34+ stem cells, genetically modifying them to overexpress the *IDS* gene, and subsequently reinfusing them into the patient. Following engraftment, these cells may differentiate into brain microglia and provide continuous CNS enzyme production without the graft-versus-host disease risks associated with allogeneic HSCT. Genome-editing strategies also represent an emerging frontier. Early clinical investigations utilizing zinc finger nucleases, such as SB-913, have explored targeted insertion of the *IDS* transgene into the highly active albumin locus of hepatocytes to facilitate durable systemic enzyme production.[8] Although initial studies have demonstrated favorable safety profiles, achieving therapeutically meaningful and sustained enzyme expression remains an important challenge requiring further optimization.

CONCLUSION

MPS II is a relentlessly progressive, multisystem disorder. The introduction of IV ERT marked a historic milestone, fundamentally altering the natural history of somatic manifestations. While standard IV ERT has transformed systemic management, addressing neurological progression remains the cornerstone of modern research. Today, the management of Hunter syndrome is at a transformative crossroads. The synergistic integration of NBS programs with breakthrough technologies—such as BBB-crossing molecular Trojan horses, ICV enzyme administration, and advanced gene therapies—holds unprecedented promise. The ultimate goal of MPS II management is shifting from mere somatic palliation toward comprehensive disease correction, aiming to preserve neurocognitive capacity and restore normal quality of life for all affected individuals.

Footnotes

Financial Disclosure: The author declared that this study received no financial support.

REFERENCES

1. Bradley LA, Haddow HRM, Palomaki GE. Treatment of mucopolysaccharidosis type II (Hunter syndrome): results from a systematic evidence review. Genet Med. 2017;19(11):1187-1201. doi: 10.1038/gim.2017.30
2. D'Avanzo F, Rigon L, Zanetti A, Tomanin R. Mucopolysaccharidosis type II: one hundred years of research, diagnosis, and treatment. Int J Mol Sci. 2020;21(4):1258. doi: 10.3390/ijms21041258
3. Ago Y, Rintz E, Musini KS, Ma Z, Tomatsu S. Molecular mechanisms in pathophysiology of mucopolysaccharidosis and pospects for innovative therapy. Int J Mol Sci. 2024;25(2):1113. doi: 10.3390/ijms25021113
4. Derrick-Roberts A, Kaidonis X, Jackson MR, et al. Comparative analysis of brain pathology in heparan sulphate storing mucopolysaccharidoses. Mol Genet Metab. 2020;131(1-2):197-205. doi: 10.1016/j.ymgme.2020.07.006
5. Ausseil J, Desmaris N, Bigou S, et al. Early neurodegeneration progresses independently of microglial activation by heparan sulfate in the brain of mucopolysaccharidosis IIIB mice. PLoS One. 2008;3(5):e2296. doi: 10.1371/journal.pone.0002296
6. Mohamed S, He QQ, Singh AA, Ferro V. Mucopolysaccharidosis type II (Hunter syndrome): clinical and biochemical aspects of the disease and approaches to its diagnosis and treatment. Adv Carbohydr Chem Biochem. 2020;77:71-117. doi: 10.1016/bs.accb.2019.09.001
7. Mao SJ, Chen QQ, Dai YL, Dong GP, Zou CC. The diagnosis and management of mucopolysaccharidosis type II. Ital J Pediatr. 2024;50(1):207. doi: 10.1186/s13052-024-01769-9
8. Ream MA, Lam WKK, Grosse SD, et al. Evidence and recommendation for mucopolysaccharidosis type II newborn screening in the United States. Genet Med. 2023;25(2):100330. doi: 10.1016/j.gim.2022.10.012

9. Burton BK, Amartino H, Giugliani R, et al. Female patients with mucopolysaccharidosis II (MPS II): insights from the hunter outcome survey. JIMD Rep. 2026;67(1):e70046. doi: 10.1002/jmd2.70046

10. Okuyama T, Tanaka A, Suzuki Y, et al. Japan Elaprase® Treatment (JET) study: idursulfase enzyme replacement therapy in adult patients with attenuated Hunter syndrome (mucopolysaccharidosis II, MPS II). Mol Genet Metab. 2010;99(1):18-25. doi: 10.1016/j.ymgme.2009.08.006

11. Lin HY, Lin SP, Chuang CK, et al. Incidence of the mucopolysaccharidoses in Taiwan, 1984-2004. Am J Med Genet A. 2009;149A(5):960-964. doi: 10.1002/ajmg.a.32781

12. Khan SA, Peracha H, Ballhausen D, et al. Epidemiology of mucopolysaccharidoses. Mol Genet Metab. 2017;121(3):227-240. doi: 10.1016/j.ymgme.2017.05.016

13. Tulebayeva A, Mukhambetova G, Sharipova M, Tylki-Szymanska A. The birth prevalence of mucopolysaccharidosis types I, II, III, IVA, VI, and VII in the Republic of Kazakhstan between 1984 and 2023. Diagnostics (Basel). 2025;15(6):679. doi: 10.3390/diagnostics15060679

14. Hao N, Yao F, Li D, et al. Long-read sequencing expands the genotypic spectrum of patients with mucopolysaccharidosis type II. J Inherit Metab Dis. 2025;48(4):e70055. doi: 10.1002/jimd.70055

15. Scarpa M, Almássy Z, Beck M, et al. Hunter Syndrome Europena Expert Council. Mucopolysaccharidosis type II: European recommendations for the diagnosis and multidisciplinary management of a rare disease. Orphanet J Rare Dis. 2011;6:72. doi: 10.1186/1750-1172-6-72

16. Malm G, Lund AM, Månsson JE, Heiberg A. Mucopolysaccharidoses in the Scandinavian countries: incidence and prevalence. Acta Paediatr. 2008;97:1577-1581. doi: 10.1111/j.1651-2227.2008.00965.x. Erratum in: Acta Paediatr. 2008;97(12):1773.

17. Ayodele O, Fertek D, Evuarherhe O, Siffel C, Audi J, Yee KS, Burton BK. A systematic literature review on the global status of newborn screening for mucopolysaccharidosis II. Int J Neonatal Screen. 2024;10(4):71. doi: 10.3390/ijns10040071

18. Krabbi K, Joost K, Zordania R, et al. The live-birth prevalence of mucopolysaccharidoses in Estonia. Genet Test Mol Biomarkers. 2012;16(8):846-849. doi: 10.1089/gtmb.2011.0307

19. Seo JH, Okuyama T, Shapiro E, Fukuhara Y, Kosuga M. Natural history of cognitive development in neuronopathic mucopolysaccharidosis type II (Hunter syndrome): Contribution of genotype to cognitive developmental course. Mol Genet Metab Rep. 2020;24:100630. doi: 10.1016/j.ymgmr.2020.100630

20. Muenzer J, Botha J, Amartino H, et al. Clinical characteristics and real-world outcomes in patients with mucopolysaccharidosis II over 18 years: final report of the hunter outcome survey. Mol Genet Metab. 2025;146(4):109284. doi: 10.1016/j.ymgme.2025.109284

21. Bhalla A, Ravi R, Fang M, et al. Characterization of fluid biomarkers reveals lysosome dysfunction and neurodegeneration in neuronopathic MPS II patients. Int J Mol Sci. 2020;21(1):5188. doi: 10.3390/ijms21155188

22. Leal GN, de Paula AC, Leone C, Kim CA. Echocardiographic study of paediatric patients with mucopolysaccharidosis. Cardiol Young. 2010;20(3):254-261. doi: 10.1017/S104795110999062X

23. Yazıcı H, Kara E, Bulut FD, et al. Genotype–phenotype correlations and shifting diagnosis age in Turkish mucopolysaccharidosis type II patients: a multicenter retrospective study. Diagnostics (Basel). 2025;15(21):2773. doi: 10.3390/diagnostics15212773

24. Tomatsu S, Pitz S, Hampel U. Ophthalmological findings in mucopolysaccharidoses. J Clin Med. 2019;8(9):1467. doi: 10.3390/jcm8091467

25. Scarpa M, Lampe C. Mucopolysaccharidosis type II. 2007 Nov 6 [updated 2026 Apr 28]. In: Adam MP, Bick S, Mirzaa GM, Wallace SE, Amemiya A, editors. GeneReviews® [Internet]. Seattle (WA): University of Washington, Seattle; 1993-2026.

26. Vollebregt AAM, Hoogeveen-Westerveld M, Kroos MA, et al. Genotype-phenotype relationship in mucopolysaccharidosis II: predictive power of IDS variants for the neuronopathic phenotype. Dev Med Child Neurol. 2017;59(10):1063-1070. doi: 10.1111/dmcn.13467

27. Li P. Molecular analyses in families with hunter syndrome indicate unequal male and female mutation rates in the iduronate-2-sulfatase gene. J Mol Genet Med. 2014;8:1000135. doi: 10.4172/1747-0862.1000135

28. Schwartz IVD, Pinto LLC, Breda G, et al. Clinical and biochemical studies in mucopolysaccharidosis type II carriers. J Inherit Metab Dis. 2009;32(6):732-738. doi: 10.1007/s10545-009-1275-9

29. Sahin O, Thompson HP, Goodman GW, Li J, Urayama A. Mucopolysaccharidoses and the blood-brain barrier. Fluids Barriers CNS. 2022;19(1):76. doi: 10.1186/s12987-022-00373-5

30. Huang L, Wu J, Tang B, et al. Efficacy of different treatment strategies in patients with mucopolysaccharidosis: a systematic review and network meta-analysis of randomized controlled trials. Orphanet J Rare Dis. 2025;20(1):211. doi: 10.1186/s13023-025-03735-y

31. Xu Y, Fang X, Luo C, et al. Allogeneic hematopoietic stem cell transplantation modulates neurodevelopmental trajectories in mucopolysaccharidosis: a longitudinal study of subtype-specific outcomes and age-dependent efficacy. Orphanet J Rare Dis. 2025;20(1):591. doi: 10.1186/s13023-025-04025-3

32. Barth AL, de Magalhães TSPC, Reis ABR, et al. Early hematopoietic stem cell transplantation in a patient with severe mucopolysaccharidosis II: a 7 years follow-up. Mol Genet Metab Rep. 2017;12:62-68. doi: 10.1016/j.ymgmr.2017.05.010

33. Sreekantam S, Smith L, Stewart C, et al. Efficacy of early haematopoietic stem cell transplantation versus enzyme replacement therapy on neurological progression in severe hunter syndrome: case report of siblings and literature review. Mol Genet Metab Rep. 2022;32:100881. doi: 10.1016/j.ymgmr.2022.100881

34. Zanetti A, Tomanin R. Targeting neurological aspects of mucopolysaccharidosis type II: enzyme replacement therapy and beyond. biodrugs. 2024;38(5):639-655. doi: 10.1007/s40259-024-00675-0

35. Sonoda H, Takahashi K, Minami K, et al. Treatment of neuronopathic mucopolysaccharidoses with blood–brain barrier-crossing enzymes: clinical application of receptor-mediated transcytosis. Pharmaceutics. 2022;14(6):1240. doi: 10.3390/pharmaceutics14061240

CASE REPORT

DOI: 10.4274/imdn.galenos.2026.2026-5

Inherit Metab Disord Nutr 2026;2:31–37

A Novel *FBXL4* Variant Presenting with Shunt-Dependent Hydrocephalus

Ayşe Nur Altun[1], Hamza Polat[2], İkbal Türker[3], Mehmet Salih Karaca[4]

[1]University of Health Sciences Türkiye, Gazi Yaşargil Training and Research Hospital, Department of Pediatrics, Division of Pediatric Metabolism Diseases, Diyarbakır, Türkiye

[2]University of Health Sciences Türkiye, Gazi Yaşargil Training and Research Hospital, Department of Medical Genetics, Diyarbakır, Türkiye

[3]University of Health Sciences Türkiye, Gazi Yaşargil Training and Research Hospital, Department of Pediatrics, Pediatric Intensive Care Unit, Diyarbakır, Türkiye

[4]University of Health Sciences Türkiye, Gazi Yaşargil Training and Research Hospital, Department of Radiology, Diyarbakır, Türkiye

Abstract

FBXL4-associated encephalomyopathic mitochondrial depletion syndrome type 13 is a very rare mitochondrial disorder. To date, more than 110 cases have been reported in the literature, and the disease presents with multisystem involvement accompanied by lactic acidosis. We aimed to expand the phenotypic spectrum by reporting a case with a previously undescribed c.1390-2A>G variant in the *FBXL4* gene and a previously unreported clinical presentation of severe hydrocephalus. The patient presented with severe lactic acidosis, developmental delay, moderate hyperammonemia, hypotonia, dysmorphic features, seizures, intrauterine growth restriction, hypertrophic cardiomyopathy, severe hydrocephalus, peripapillary atrophy, and encephalopathy. We aimed to contribute to the literature by identifying a new splice-site variant and the severe clinical presentation associated with it, thereby expanding the phenotypic spectrum, and by deepening understanding of the genotype-phenotype relationship of splice-site mutations.

Keywords: *FBXL4* gene, Mitochondrial depletion syndromes, Lactic acidosis, Hydrocephalus

INTRODUCTION

Mitochondria are organelles involved in cellular energy production and apoptosis. Mitochondrial proteins are encoded by both nuclear and mitochondrial DNA. Most of these proteins are encoded by nuclear DNA, which is thought to contain between 1,000 and 1,500 genes. *F-box and leucine-rich repeat protein 4* (*FBXL4*) is a mitochondrial protein localized to the intermembrane space, encoded by the nuclear *FBXL4* (MIM#605654) gene, and is a member of the F-box protein family. The F-box portion of the protein interacts with the Skp1 adaptor to assemble the Skp1-Cullin1-F-box E3 ubiquitin ligase complex, which ubiquitinates the mitophagy receptors BNIP3 and NIX, leading to their degradation and suppression of mitophagy.[1-3]

FBXL4-associated disease was first described in 2013. In these studies, it was noted that the *FBXL4* protein was localized between the inner and outer mitochondrial membranes, and that impairment of its function resulted in mtDNA depletion, mitochondrial structural abnormalities, and reduced activity of oxidative phosphorylation enzymes.[2,3] Common clinical manifestations of the disease, defined as *FBXL4*-associated encephalomyopathic mitochondrial depletion syndrome type 13, include hypotonia, lactic acidosis, growth retardation, facial dysmorphism, malnutrition, and cerebral atrophy. Although less frequent, the following manifestations are also observed: microcephaly, hyperammonemia, nystagmus, strabismus, optic atrophy, cardiac involvement, and seizures.[4] While hydrocephalus has previously been reported, no case of severe hydrocephalus necessitating ventriculoperitoneal (VP) shunt placement has been described to date.

Address for Correspondence: Ayşe Nur Altun, MD, University of Health Sciences Türkiye, Gazi Yaşargil Training and Research Hospital, Department of Pediatrics, Division of Pediatric Metabolism Diseases, Diyarbakır, Türkiye

E-mail: draysenuraltun@gmail.com **ORCID ID:** orcid.org/0000-0003-2561-2516

Received: 15.05.2026 **Accepted:** 16.07.2026 **Publication Date:** 05.10.2026

Cite this article as: Altun AN, Polat H, Türker İ, Karaca MS. A novel *FBXL4* variant presenting with shunt-dependent hydrocephalus. Inherit Metab Disord Nutr. 2026;2:31–37

Copyright© 2026 The Author(s). Published by Galenos Publishing House on behalf of Child Nutrition Metabolism Association.
This is an open access article under the Creative Commons AttributionNonCommercial 4.0 International (CC BY-NC 4.0) License.

CASE REPORT

The patient, a 34-month-old boy, was born at term by cesarean section to a 36-year-old mother from a 1st cousin marriage. His four siblings do not have any health problems. Elevated lactate levels were detected at 6 months of age. Thiamine 100 mg/day, riboflavin 100 mg/day, coenzyme Q10 100 mg/day, biotin 10 mg/day, and sodium benzoate 250 mg/kg/day were started on suspicion of mitochondrial disease.

The patient's body weight was 10 kg [standard deviation score (SDS)≤−3.0], height was 92 cm (SDS −1.88), and head circumference was 51 cm (SDS +0.28). He had growth retardation, developmental delay, hypotonia, and dysmorphic features. Dysmorphic features included a prominent forehead, a long, smooth philtrum, retrognathia, micrognathia, thick eyebrows, upslanting palpebrae, long eyelashes, and a thin upper lip (Figure 1).

Laboratory examination revealed a mild elevation of aspartate aminotransferase (116 U/L; maximum level of 225 U/L). The acylcarnitine profile was normal. Analysis of plasma amino acid levels revealed an elevated alanine concentration of 1302 µmol/L [reference range (RR): 157-481]. Urine organic acid analysis revealed elevated levels of pyruvic acid (108 Mmol/molcre; RR: 0-32), lactic acid (364 Mmol/molcre; RR: 0-60), 2-ketoglutaric acid (209 Mmol/molcre; RR: 0-136), 3-hydroxybutyric acid (108 Mmol/molcre; RR: 0-63), 3-hydroxyisobutyric acid (108 Mmol/molcre; RR: 0-28), and 2-hydroxybutyric acid (6.4 Mmol/molcre; RR: 0.03-1.8). Lactate levels ranged from 3.2 to 17.1 Mmol/L (RR: 0-2). Ammonia levels were between 57 and 243 mcg/dL (RR: 31-123). Eye examination revealed peripapillary atrophy, whereas echocardiography showed left ventricular hypertrophy.

Imaging performed at 3 months of age showed dilatation of both lateral ventricles (left, 25 mm; right, 23 mm) and mild dilatation of the 3rd and 4th ventricles. Because the diagnosis remained unclear, the ventricular dilation identified on previous cranial magnetic resonance imaging (MRI) did not fully explain the clinical picture; hypotonia and developmental delay persisted, and lactic acidosis raised suspicion for an underlying mitochondrial disorder. A repeat cranial MRI was performed at 2 years and 10 months of age. Cranial MRI showed severe tetraventricular hydrocephalus. Bilateral cortical sulci were partially effaced. The corpus callosum was hypoplastic. Genetic analysis revealed a homozygous c.1390-2A>G variant in the *FBXL4* gene (rs1263785322) (Figure 2). The variant has not been reported in the homozygous state in gnomAD Exomes, 1000 Genomes, ESP6500, and ExAC databases. The variant was classified as likely pathogenic because it met the PVS1 and PM2 criteria of the ACMG variant classification.

The patient underwent VP shunting for hydrocephalus at the age of 39 months. A postoperative cranial computed tomography scan showed severely dilated ventricles and a VP shunt (Figure 3). Phenytoin was started preoperatively as prophylaxis. After the shunt operation, we admitted the patient because of malnutrition and metabolic acidosis. The patient received nasogastric tube feeding. Sodium alginate and pantoprazole were initiated for vomiting in a patient with FBXL4-associated encephalomyopathic mitochondrial depletion syndrome type 13. Electroencephalography performed at the 3rd postoperative month was compatible with both a highly active, multifocal epileptic disorder and cerebral dysfunction.



Figure 1. (a, b) Prominent forehead, long and smooth philtrum, micro-retrognathia, thick eyebrows, upslanting palpebra, long eyelashes, thin upper lip.

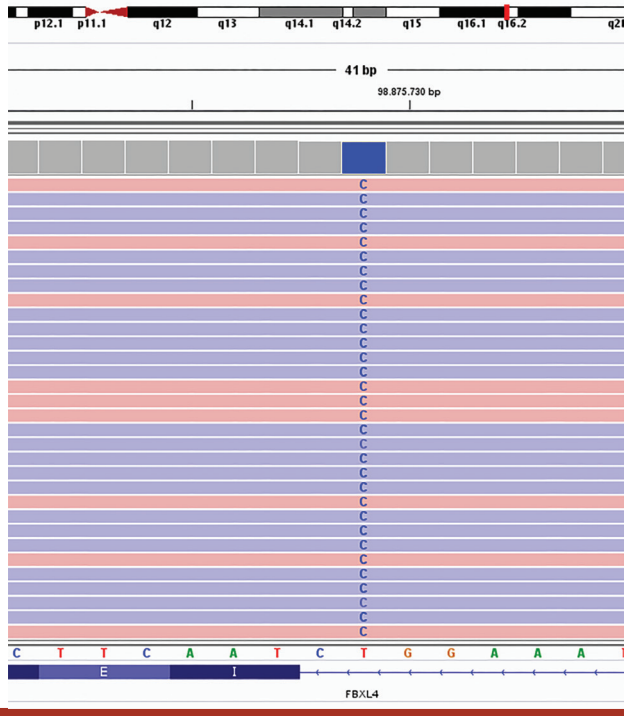


Figure 2. Integrative Genomics Viewer visualization of c.1390-2A>G variant.

MR spectroscopy performed at the 3rd postoperative month showed no lactate peak in a single-voxel view with a medium-length TE in the thalamic region of the deep gray matter; no peak was detected in other regions (Figure 4). MRI performed at 6 months postoperatively showed enlarged ventricles and diffuse, symmetric, mild signal enhancement in the thalamus, nucleus caudatus, and lentiformis on the T2 series (Figure 5). In the same imaging series, signal enhancement was observed in the brainstem at the level of the middle cerebellar peduncles (Figure 6).



Figure 3. Enlarged lateral ventricules and shunt catheter after VP shunt operation.

VP, ventriculoperitoneal.

A cerebrospinal fluid culture performed because of encephalopathy revealed growth of vancomycin-sensitive *Staphylococcus epidermidis*. Appropriate antibiotic therapy was initiated. An external ventricular drain was placed, antibiotic therapy was initiated, and topiramate, levetiracetam, and clonazepam were added to the treatment regimen for seizures and dystonic contractions. Proteinuria was detected. Blood gas analysis revealed a pH of 6.89, a pCO_2 of 88 mmHg, an HCO_3 of 16.6 mg/dL, and a lactate of 14.5 Mmol/L; sodium dichloroacetate was administered at 50 mg/kg/day, and hemodialysis was therefore performed. He died of sepsis and encephalopathy at 45 months of age (Table 1).

Method

From the patient, 2 mL of peripheral blood was collected in EDTA tubes and stored at −20 °C. Genomic DNA was isolated from peripheral blood leukocytes using QIAamp DNA Blood Mini QIAcube Kit (Qiagen, Hilden, Germany) according to the manufacturer's protocols. All coding exons and exon-intron boundaries of 4493 genes were amplified using the Clinical Exome Solution v2 kit (SOPHiA Genetics, Boston, USA).

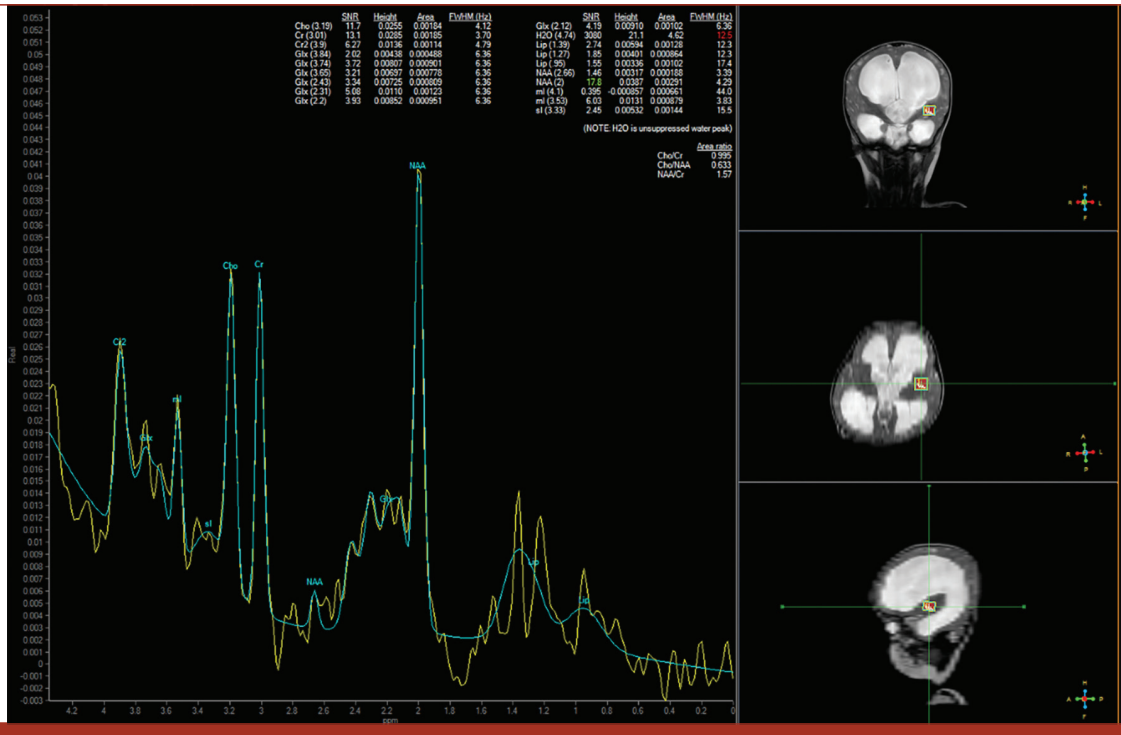


Figure 4. Brain MR spectroscopic imaging of the patient at the 3rd postoperative month revealed lactate peak on single-voxel MR spectroscopy with a medium-length TE in the thalamic region of the deep gray matter.

MR, magnetic resonance.

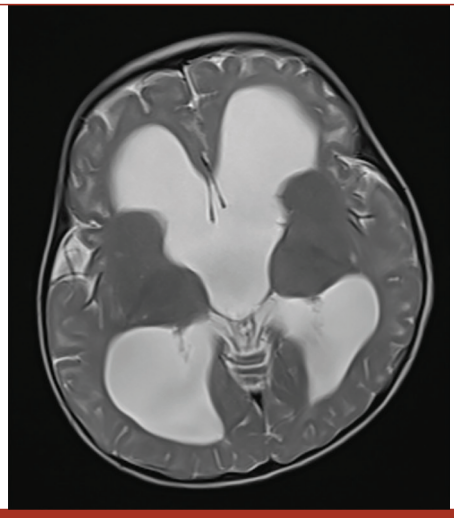


Figure 5. Enlarged ventricles and diffuse, symmetric mild signal enhancement in the thalamus, nucleus caudatus and lentiformis in T2 series.



Figure 6. Signal enhancement in the brain stem at the level of the middle cerebellar peduncles.

Table 1. Chronological timeline of the patient's clinical course.

Age	Clinical findings/investigations	Management
3 months	Cranial MRI: Dilatation of both lateral ventricles and mild dilatation of the third and fourth ventricles.	
6 months	Persistent hyperlactatemia and hyperammonemia detected; mitochondrial disease suspected.	Mitochondrial support and sodium benzoate treatment was initiated.
34 months	Growth retardation, developmental delay, hypotonia, dysmorphic features, persistent lactic acidosis, hyperalaninemia, intermittent hyperammonemia, peripapillary atrophy, and left ventricular hypertrophy. Repeat cranial MRI: severe tetraventricular hydrocephalus and hypoplasia of the corpus callosum. Genetic test: Homozygous *FBXL4* c.1390-2A>G likely pathogenic variant.	Metabolic investigations performed. Molecular diagnosis of *FBXL4*-associated encephalomyopathic mitochondrial DNA depletion syndrome established.
39 months	Progressive hydrocephalus.	Ventriculoperitoneal (VP) shunt placement; prophylactic phenytoin initiated.
42 months (3 months after VP shunt)	EEG showed highly active multifocal epileptic disorder with cerebral dysfunction. MR spectroscopy demonstrated a mild lipid-lactate peak in the bilateral thalami.	Antiepileptic treatment continued.
45 months (6 months after VP shunt)	Follow-up MRI showed persistent ventricular enlargement and new bilateral symmetric T2 hyperintensities involving the thalami, caudate nuclei, lentiform nuclei, and brainstem (middle cerebellar peduncles).	
45 months	Encephalopathy; CSF analysis: *Staphylococcus epidermidis*. Proteinuria, severe metabolic acidosis (pH 6.89, lactate 14.5 mmol/L), sepsis, seizures, and dystonic contractions developed.	External ventricular drainage, targeted antibiotic therapy, topiramate, levetiracetam, clonazepam, sodium dichloroacetate, and hemodialysis were administered. The patient died at 45 months of age.

MRI, magnetic resonance imaging; CSF: cerebrospinal fluid.

The prepared library was sequenced on the Illumina NextSeq platform (Illumina Inc., San Diego, CA, USA). The data were analyzed using SOPHiA DDM software (SOPHiA Genetics, Boston, USA) in conjunction with clinical findings. Informed consent for diagnostic and research studies was obtained from the patients' parents in accordance with the Declaration of Helsinki protocols.

DISCUSSION

Dysfunction of *FBXL4* leads to defects in mitochondrial fusion, mitophagy, and mitochondrial DNA maintenance, resulting in encephalomyopathic- type mitochondrial DNA depletion syndrome 13. The disease was first described in 2013 in two distinct patient groups, and more than 110 cases have been reported so far.[5-22] In addition to the typical clinical presentation, findings, including small for gestational age, short stature, and feeding difficulties, have been described in the literature.[4]

Although microcephaly is present in approximately half of the patients reported in the literature, our patient has relative macrocephaly. Antenatal hydrocephalus was reported in only 1 patient, whereas dilated ventricles are more frequently reported in the literature.[4,12,18,19,20] No patients have been reported in the literature with an indication for VP shunt due to severe hydrocephalus. Postoperatively, the patient experienced seizures and dystonia. It is unclear whether this was operation-related or related to the disease course.

Although the age of disease onset has been reported to range from the intrauterine period to 3 months of age, our patient's delayed presentation may be attributable to compensated lactic acidosis. Additionally, the impact of socioeconomic factors on delayed admission cannot be overlooked. However, it is possible that he did not experience an episode of lactic acidosis or hyperammonemia prior to his first admission, or that any episode was not severe enough to be noticed.

To date, survival in this disease is variable: the median age at death is two years (range: 2 days-75 months), although individuals surviving to 36 years of age have been reported.[23] It has also been reported that survival time is longer in individuals with missense variants than in those with null variants.[4]

To date, 6 splice-site mutations have been reported[4,24,25,26] In a case with a homozygous splice-site pathogenic variant, symptoms appeared on the first day of life; hyperammonemia, hearing loss, and cardiac findings were observed, findings that are reported in less than 50% of patients in reviews, and the patient died at 23 months of age.[26] In another case in which a compound-heterozygous splice-site pathogenic variant was reported, the age of onset was in the neonatal period, as in the previous case, and the patient was 4 years old and alive at the time of publication.[25] Detailed clinical information about patients with other splice-site variants could not be obtained.[4,24] Therefore, the relationship between splice-site variants and phenotypes could not be evaluated. However, upon examining patients with the described clinical findings, we do not have sufficient data to conclude that variants in the joint region are associated with early-onset disease. The c.1390-2A>G homozygous variant in the *FBXL4* gene identified in our patient represents a novel splice-site alteration between exons 7 and 8 that has not been reported previously. The more severe clinical findings observed in patients with splice-site variants may be due to these variants exerting a more deleterious effect on proteins through exon skipping, intron retention, and activation of cryptic splice sites. The c.1390-2A>G variant detected in this case can directly disrupt a critical splice site in the gene, leading to complete inhibition of protein synthesis or defective protein synthesis. This changes the acceptor splice site from the consensus sequence, thereby interfering with splicing.

Cranial MR imaging of the patient showed cerebral atrophy, involvement of the basal ganglia and white matter,a thin corpus callosum, and hydrocephalus, findings that are consistent with the literature. The finding that distinguishes the patient from the literature is that he had hydrocephalus severe enough to require shunt insertion. In addition, although less commonly reported in the literature, our patient had brainstem involvement, and no lactate peak was detected on MR spectroscopy despite high lactate levels.[4,24]

During follow-up, the patient's encephalopathic periods were not always accompanied by lactic acidosis. This suggests that central nervous system manifestations of the disease are risk factors independent of its prognosis. Moreover, clinical deterioration associated with elevated lactic acid levels worsened during catabolic processes such as dehydration, infection, and surgery, making the patient's externalization difficult.

Furthermore, the history of SGA birth and dysmorphic features, observed in most patients described in the literature, may indicate that the *FBXL4* gene is also active during the intrauterine period.[17,18,24]

Study Limitations

A key limitation of this report is that genetic testing was limited to a targeted panel of 4,493 genes rather than whole-exome or whole-genome sequencing. An additional genetic diagnosis contributing to the unusually severe hydrocephalus phenotype cannot be ruled out; a dual diagnosis remains possible. This limitation is explicitly acknowledged because further genomic studies are unavailable.

CONCLUSION

We aimed to contribute to phenotyping by reporting a patient with a novel variant in the *FBXL4* gene and a previously unreported clinical finding. Further studies and additional case reports are needed to clarify the function of FBXL4 and to improve phenotyping.

Ethics

Informed Consent: Informed consent for diagnostic and research studies was obtained from the patients' parents in accordance with the Declaration of Helsinki protocols.

Footnotes

Authorship Contributions

Surgical and Medical Practices: İ.T., M.S.K., Concept: A.N.A., Design: A.N.A., Data Collection or Processing: A.N.A., H.P., M.S.K., Analysis or Interpretation: A.N.A., H.P., Literature Search: A.N.A., Writing: A.N.A.

Conflict of Interest: The author(s) have no conflicts of interest to declare.

Financial Disclosure: The author(s) declared that this study received no financial support.

REFERENCES

1. Cao Y, Zheng J, Wan H, et al. A mitochondrial SCF-FBXL4 ubiquitin E3 ligase complex degrades BNIP3 and NIX to restrain mitophagy and prevent mitochondrial disease. EMBO J. 2023;42(13):e113033. doi:10.15252/embj.2022113033
2. Bonnen PE, Yarham JW, Besse A, et al. Mutations in FBXL4 cause mitochondrial encephalopathy and a disorder of mitochondrial DNA maintenance. Am J Hum Genet. 2013;93(3):471-481. doi: 10.1016/j.ajhg.2013.07.017
3. Gai X, Ghezzi D, Johnson MA, et al. Mutations in FBXL4, encoding a mitochondrial protein, cause early-onset mitochondrial encephalomyopathy. Am J Hum Genet. 2013;93(3):482-495. doi: 10.1016/j.ajhg.2013.07.016
4. El-Hattab AW, Craigen WJ, Scaglia F. Mitochondrial DNA maintenance defects. Biochim Biophys Acta. 2017;1863(6):1539-1555. doi: 10.1016/j.bbadis.2017.02.017
5. Ballout RA, Al Alam C, Bonnen PE, Huemer M, El-Hattab AW, Shbarou. *FBXL4*-related mitochondrial DNA depletion syndrome 13 (MTDPS13): a case report with a comprehensive mutation review. Front Genet. 2019;10:39. doi: 10.3389/fgene.2019.00039
6. Kuptanon C, Srichomthong C, Ittiwut C, et al. Whole exome sequencing revealed mutations in FBXL4, UNC80, and ADK in Thai patients with severe intellectual disabilities. Gene. 2019;696:21-27. doi: 10.1016/j.gene.2019.01.049
7. Nardi N, Proulx F, Brunel-Guiton C, Oligny LL, Piché N, Mitchell GA, Joyal JS. Fulminant necrotizing enterocolitis and multiple organ dysfunction in a toddler with mitochondrial DNA depletion syndrome-13. J Pediatr Intensive Care. 2020;9:54-59. doi: 10.1055/s-0039-1697620
8. Hu C, Li X, Zhao L, Shi Y, Zhou S, Wu B, Wang Y. Clinical and molecular characterization of pediatric mitochondrial disorders in south of China. Eur J Med Genet. 2020;63(8):103898. doi: 10.1016/j.ejmg.2020.103898
9. Köse E, Köse M, Edizer S, Akışın Z, Yılmaz ZB, Şahin A, Genel F. Different clinical presentation in a patient with two novel pathogenic variants of the FBXL4 gene. Turk J Pediatr. 2020;62(4):652-656. doi: 10.24953/turkjped.2020.04.016
10. Emperador S, Garrido-Pérez N, Amezcua-Gil J, et al. Molecular characterization of new FBXL4 mutations in patients with mtDNA depletion syndrome. Front Genet. 2019;10:1300. doi: 10.3389/fgene.2019.01300
11. Bychkov IO, Itkis YS, Tsygankova PG, et al. Mitochondrial DNA maintenance disorders in 102 patients from different parts of Russia: mutational spectrum and phenotypes. Mitochondrion. 2021;57:205-212. doi: 10.1016/j.mito.2021.01.004
12. Oncul U, Kose E, Eminoglu FT. A mild phenotype of mitochondrial DNA depletion syndrome type 13 with a novel *FBXL4* variant. Mol Syndromol. 2021;12(5):294-299. doi: 10.1159/000515928
13. İnci A, Aktaş E, Cengiz Ergin FB, Okur İ, Biberoğlu G, Ezgü FS, Tümer L.The first case with FBXL4 mutation successfully treated with a parenteral ketogenic diet for lactic acidosis. JPEN J Parenter Enteral Nutr. 2021;45(8):1788-1792. doi: 10.1002/jpen.2121
14. Saini N, Vijayasree V, Nandury EC, Dalal A, Aggarwal S. Prenatal phenotype of FBXL4-associated encephalomyopathic mitochondrial DNA depletion syndrome-13. Nat Diagn. 2022;42(13):1682-1685. doi: 10.1002/pd.6272
15. Alotaibi M, Alqasmi A, Albassam F, Alkahtani T, Alqahtany M, Alkhaldi M. The first reported case of a child with two different rare metabolic disorders: very long-chain acyl-coa dehydrogenase deficiency and encephalomyopathic mitochondrial DNA depletion syndrome 13. Glob Med Genet. 2023;10(4):278-281. doi: 10.1055/s-0043-1775979
16. Fellner A, Wali GM, Mahant N, et al. Genome sequencing reanalysis increases the diagnostic yield in dystonia. Parkinsonism Relat Disord. 2024;124:107010. doi: 10.1016/j.parkreldis.2024.10701
17. Kahraman AB, Çelik H, Bagci Z, Sezer A, Kılıç M. FBXL4-related encephalomyopathic mitochondrial DNA depletion syndrome: a rare cause of hyperammonemia. Mol Genet Metab Rep. 2025;43:101206. doi: 10.1016/j.ymgmr.2025.101206
18. Akiba T, Shimada S, Matsuda S, et al. Siblings of FBXL4-related mitochondrial DNA depletion syndrome, leading to fatal fulminant pneumonia. Mol Genet Metab Rep. 2025;45:101266. doi: 10.1016/j.ymgmr.2025.101266
19. Zhai Y, Chen J, Yang S, Wang H, Xiao Y, Liu S. Prenatal diagnosis of a compound heterozygous variation in the *FBXL4* gene by trio-WES and imaging monitoring: a case report. Front Genet. 2025;16:1539288. doi: 10.3389/fgene.2025.1539288
20. D'Amato G, Gentile M, Carella R, Giannini A, Faienza MF, Tummolo A. The ketogenic diet in the neonatal intensive care setting: the case of a preterm newborn with mitochondrial DNA depletion syndrome type 13 (MTDPS13). Case Rep Genet. 2026;2026:6492770. doi: 10.1155/crig/6492770
21. Ros A, Hurtado I, Vázquez-Méndez É, et al. Prenatal FBXL4-associated mitochondrial DNA depletion syndrome-13: a new case and review of the literature. Prenat Diagn. 2025;45(6):829-834. doi: 10.1002/pd.6794
22. Keser M, Demirci B, Uçar HK, Anlaş Ö, Arslan İ, Gürbüz BB. A patient with organic acidemia, hyperammonemia, and a *FBXL4* variant suggesting mitochondrial DNA depletion syndrome. Mol Syndromol. 2026;17(1):67-73. Erratum in: Mol Syndromol. 2025;1. doi: 10.1159/000545585
23. Almannai M, Dai H, El-Hattab AW, Wong LJC. *FBXL4*-related encephalomyopathic mitochondrial DNA depletion syndrome. 2017. In: Adam MP, Bick S, Mirzaa GM, Wallace SE, Amemiya A, editors. GeneReviews® [Internet]. Seattle (WA): University of Washington, Seattle; 1993-2026. Accessed July 26, 2025. https://www.ncbi.nlm.nih.gov/books/NBK368609/
24. Huemer M, Karall D, Schossig A, et al. Clinical, morphological, biochemical, imaging and outcome parameters in 21 individuals with mitochondrial

maintenance defect related to FBXL4 mutations. J Inherit Metab Dis. 2015;38(5):905-914. doi: 10.1007/s10545-015-9836-6

25. Pronicka E, Piekutowska-Abramczuk D, Ciara E, et al. New perspective in diagnostics of mitochondrial disorders: two years' experience with whole-exome sequencing at a national paediatric centre. J Transl Med 2016;14(1):174. doi: 10.1186/s12967-016-0930-9

26. Dai H, Zhang VW, El-Hattab AW, et al. FBXL4 defects are common in patients with congenital lactic acidemia and encephalomyopathic mitochondrial DNA depletion syndrome. Clin Genet. 2017;91(4):634-639. doi: 10.1111/cge.12894